Describing the chemical bonding in C70 and C70O3 - a quantum chemical topology study

Describing the chemical bonding in C_{70} and $C_{70}O_3$ – a quantum chemical topology study.

Andrzej Bil,*[,a,b], Zdzisław Latajka,[b] Jürg Hutter,[a] Carole A. Morrison[c]

[a] ***Institute of Physical Chemistry, University of Zürich, Winterthurerstrasse 190, CH-8057 Zürich, Switzerland***

[b] ***Faculty of Chemistry, University of Wrocław F. Joliot Curie 14, 50-383 Wrocław Poland***

[c] ***School of Chemistry and EaSTCHEM Research School, The University of Edinburgh, King's Buildings, West Mains Road, Edinburgh, EH9 3JJ, UK***

**** abil@elrond.chem.uni.wroc.pl***

Keywords: fullerene; molozonides; AIM; ELI-D; reaction mechanism

Abstract:

An essential factor in accounting for the chemical properties of C_{70} is the delocalization of 70 π electrons throughout the structure. C_c-C_c and C_a-C_b bonds have dominant characteristics of double bonds, whereas the remaining six other types of bonds are best viewed as single bonds with contributions from π-electron density, the size of which depends on the identity of the bond. 'Single' bonds can act as active sites in chemical reactions which would typically require a multiple bond, such as addition of an ozone molecule, due to the fact that all adjacent bonds can serve as an efficient source of π-electron density. Thus any alteration in the electron density distribution following functionalization has far-reaching impact. We note that formation of the most stable ozonide isomer causes the smallest total perturbation in the electron density of the parent fullerene. C-C bond evolution, traced by the topological analysis of the electron localizability indicator, correlates well with the shape of the minimum energy path for the ozone ring opening reaction on the fullerene surface, and that cleavage of the covalent C-C bond is detected at the transition state of the reaction. Finally, we observe that the O-O bond in $C_{70}O_3$ is protocovalent, and as such resembles the O-O bond in H_2O_2.

Introduction

The fullerene C_{70} contains five types of carbon atom, typically labeled a to e, where a refers to atoms in the apical layer and e to atoms in the equatorial belt (**Figure 1**). As a consequence, the molecule has eight types of chemical bonds, half of which lie at the fusion of six-member rings (C_a-C_b, C_c-C_c, C_d-C_e and C_e-C_e bonds), while the remaining four (C_a-C_a, C_b-C_c, C_c-C_d, and C_d-C_d) are at the fusion of five- and six-member rings.

It is widely assumed that the C_a-C_b and C_c-C_c bonds, which are the [6,6] bonds near the poles of the fullerene, have significant double bond character.[1] Such a point is rooted in experimental findings, e.g. the addition reaction between an ozone molecule and C_{70} leads exclusively to the molozonide products a,b-$C_{70}O_3$ and c,c-$C_{70}O_3$ (see **Figure 2** for the structure of molozonides). Derivatization of a double bond in C_{70} should lead to a product with a single bond between the sp^3-hybridized carbon atoms in the cage. It stands to reason that the electronic structure of the product must be entirely different from the parent structure, as the π electrons from the double bond are now associated with the newly formed bonds. As a consequence, UV-VIS spectra of the a,b and c,c derivatives of C_{70} should be different from the spectra of the parent fullerene. This has been observed, not only for the a,b-$C_{70}O_3$, c,c-$C_{70}O_3$ molozonides, but also for the a,b-$C_{70}O$ and c,c-$C_{70}O$ epoxides (**Figure 2**), which are the products that result from thermolysis of the molozonides.[1]

Experiment has found that formation of a,a-$C_{70}O$, b,c-$C_{70}O$, c,d-$C_{70}O$ and d,d-$C_{70}O$ oxides leads to oxidoannulenes (**Figure 2**), where the carbon-carbon bond is broken upon oxide formation, in contrast to the epoxide structure (C-C bond retained) for a,b-$C_{70}O$ and c,c-$C_{70}O$.[1] This supports the opinion that [5,6] bonds, which are longer than the [6,6] C_a-C_b and C_c-C_c bonds, have single bond character. Derivatization of C_{70} which leads to breaking of these bonds is expected to retain the system of 70 π electrons, and as a consequence, the UV-VIS spectra of $C_{70}O$ oxidoannulenes would be expected to share characteristic features with the spectrum of the parent fullerene.

Heymann points out that the alteration of the C-C bond length near to the fullerene poles is larger than for the equatorial bonds. He concludes that the latter ones should be more aromatic and that their derivatization should lead to more noticeable perturbations in the π-electron system.[1] For the time being, however, there is no experimental evidence for the existence of the e,d or e,e isomers of C_{70} oxides or molozonides.

Our previous theoretical calculations[2] indicate that isomers a,b-$C_{70}O$ and c,c-$C_{70}O$ are epoxides, whereas all others, including the hypothetical (i.e. chemically inaccessible) d,e and

e,e isomers, conform to the open oxidoannulene form, which is in line with experimental findings. We also considered all existing and *a priori* possible isomers of $C_{70}O_3$. This lead us to eight minima on the potential energy surface, with a,b-$C_{70}O_3$ and c,c-$C_{70}O_3$ being the most stable and e,e-$C_{70}O_3$ the least stable. According to our calculations, all isomers apart from e,e-$C_{70}O_3$ remains stable at room temperature. For e,e-$C_{70}O_3$ we observed a spontaneous ozone ring opening reaction during the course of a molecular dynamics (MD) run (see **Figure 2** for the structure of the product). Similar results were obtained in a MD study of $C_{70}O_3$ isomers doped endohedrally with noble gas atoms[3] and light molecules.[4]

Molozonides are formed through a dipolar 1,3 cycloaddition reaction over a double (multiple) bond.[5,6] Interestingly, all eight theoretically possible molozonides we obtained share a closed structure, which means that addition of a O_3 molecule to C_{70} does not lead to the cleavage of any carbon-carbon bond. This suggests that limiting the discussion of chemical properties of C_{70} to single or double bonds is too simple. It seems that C-C bonds, which in some reactions exhibit properties typical for single bonds can, in other reactions, behave in ways more expected for double bonds. The available evidence for bond delocalization in C_{70} comes from experiments where adducts are formed to bonds other than C_a-C_b or C_c-C_c. A good example is a reaction with benzyne, where a,b, c,c, d,d and d,e monoadducts are formed in the ratio 42:35:13:10 .[7]

In this paper we have undertaken to study the problem of the C-C bond properties in C_{70} in the context of molozonide formation. To address this issue we have used quantum chemical topology methods. We have performed a series of topological analyses of the electron densities and electron localizability indicators calculated for all relevant molecules. Topological analyses, as originally described by Bader, quantitatively define and characterize bonding interactions directly from the electron density.[8] The electron localizability indicator (ELI-D)[9,10] uses many similar constructs to those defined by Bader, but specifically yields chemical interpretation based on core, bonding and non-bonding electron pairs.[11] It is therefore particularly useful to evidence and describe properties of covalent bonds. As an example, in **Figure 3** we present a spatial layout of the localization domain of an ELI-D for a,b-$C_{70}O_3$.

This methodology also allows us to trace bond evolution in the course of a chemical reaction.[12] As mentioned above, for e,e-$C_{70}O_3$ we have previously observed a spontaneous ozone ring opening reaction in the course of a MD run at room temperature. The two

experimentally known molozonides, a,b-$C_{70}O_3$ and c,c-$C_{70}O_3$, decompose thermally to O_2 and the proper oxide.[1] The details of the mechanism of this reaction is unknown. As discussed in our previous paper, it seems that the ozone ring opening reaction on the fullerene surface is the first step of the thermolysis.[2] Contrary to the e,e-$C_{70}O_3$ isomer, for a,b-$C_{70}O_3$ and c,c-$C_{70}O_3$, the calculated energy barriers for the ring opening process are large, at 20.8 kcal mol^{-1} and 24.3 kcal mol^{-1} respectively.[2] These numbers are in good agreement with the experimental values of the thermolysis activation energy (22.6 kcal mol^{-1} for a,b-$C_{70}O_3$, 24.4 kcal mol^{-1} for c,c-$C_{70}O_3$).[1] In this account we address the mechanism of the ozone ring opening in experimentally known a,b-$C_{70}O_3$ and c,c-$C_{70}O_3$ as well as the hypothetical e,e-$C_{70}O_3$ isomer from the point of view of topological methods.

The paper is organized as follow. First we discuss the properties of the bonds in C_{70}. In the next section we report how an O_3 molecule or oxygen atom modifies the C-C bond properties when attached to the C_{70} surface. Then we discuss potential factors influencing the relative stability of the ozonide isomer series. Finally, we analyze bond evolution in the course of the ozone ring opening for the a,b-, c,c- and e,e- isomers of $C_{70}O_3$.

Methods

Geometry optimizations were performed using the Becke-Lee-Yang-Parr exchange-correlation functional,[13,14] coupled to a Gaussian and plane-wave basis set,[15] as implemented in the QUICKSTEP program,[16] which is part of the CP2K suite of software.[17] The functional was coupled to the semi-empirical DFT-D3 dispersion correction proposed by Grimme.[18] We used the Goedecker-Teter-Hutter norm-conservative pseudopotentials optimized for use against the BLYP functional, available with the CP2K distribution.[19] Valence orbitals of all elements were expanded using DZVP-GTH-BLYP double-zeta quality basis sets. The energy cutoff of 350Ry was used to define an auxiliary basis set, together with the cubic periodic boundary conditions to create a simulation cell of length 20 Å. Minimum energy pathways for the ozone ring opening reaction in a,b-$C_{70}O_3$, c,c-$C_{70}O_3$ and e,e-$C_{70}O_3$ were obtained using the improved tangent nudged elastic band method (NEB).[20]

Information on the nature of bonding interactions has been obtained from a topological analysis of the electron density and from the computed electron localizability indicator (ELI-D). Introduced by Bader in his concept of "atoms in molecules" (AIM),[8] this framework provides a formal definition of a chemical bond. The classification of a bonding interaction is based on the numerical values of the electron density (ρ), the Laplacian of the electron density

(Δρ), the total energy density (H), and the ellipticity (ε) at the (3,-1) bond critical point (bcp), which is a saddle point on the electron density (i.e. a minimum with respect to the interatomic path and a maximum along the perpendicular directions). The topological analysis provided by Becke and Edgecombe's electron localization function (ELF),[21] which applies also to the electron localizability indicator (ELI-D), has been proposed by Silvi and Savin.[22] This method provides a tool to partition the molecular space into core and valence attractor basins, from which we can calculate integral properties, such as an average electron population or a volume. Loosely speaking, the ELI-D is proportional to the charge needed to form a same-spin electron pair.[11] In the context of the Hartree-Fock approximation, the ELI-D resembles Becke and Edgecombe's ELF, but without a reference to the uniform electron gas.[10] As a consequence, the ELI-D has the same topology as the ELF for a single determinant wavefunction.

The molecular orbitals necessary to compute the electron density or the ELI-D have been calculated with the B3LYP functional coupled to a triple-zeta quality TZVP basis set,[23] as implemented in the software package TURBOMOLE.[24] Topological analysis of ρ(r) and ELI-D(r) has been performed using the Dgrid program.[25]

Results.

Bond properties in C_{70}.

In **Table 1** we have collected parameters that characterize the bonding situation in the parent fullerene, specifically: bond length, electron population of the valence V(C,C) ELI-D basin, as well as parameters calculated at the C-C bond critical point (the electron density, the Laplacian of the electron density, ellipticity and the energy density). According to AIM theory, the presence of a (3,-1) bcp on the interatomic line linking two atoms in a molecule in the equilibrium geometry indicates that a bonding interaction is present. A typical covalent bond is characterized by a large value for the electron density at the bcp and large negative values for the Laplacian of the electron density and the energy density. The existence of a valence disynaptic basin in the ELI-D or ELF between two atoms is considered to indicate that the bond is dominated by covalent interactions. Integrating the electron density over the basin yields the bond population. Thus strong, multiple covalent bonds are expected to have larger basin populations.

Note that a description of chemical bonding based on real-space quantum chemical topology methods is self-contained, and in principle does not require reference to orbital models that categorise electrons as π or σ , or semi-empirical concepts such as a bond order. However, as demonstrated in the introduction, earlier papers, especially those discussing experimental findings of C_{70} and its derivatives, refer extensively to the concepts of single or double bonds and the delocalization of 70 π-electrons to rationalize the properties and reactivity of the fullerene surface. It therefore seems justifiable to interpret the real space topology results derived in this work using these widespread terms, as it places the conclusions in the broader context of existing literature. For a molecule such as C_{70}, which comprises C-C bonds that have properties between the limiting cases of purely single or purely double bond, such an interpretation is possible[8] and is quite straightforward. In **Table 1** we list the data obtained for C-C bonds present in ethane, ethene and benzene, as reference data for systems with typical single, double and delocalized bonds in an aromatic system. The reference data allow us to classify any bond in C_{70}.

An increasing strength of the heavy-atom bonds in CH_3-CH_3, C_6H_6 and CH_2=CH_2 is reflected by the decreasing bond length R, the energy density H and the Laplacian of the electron density Δρ, as well as an increasing electron density (ρ) at the bcp and the total basin populations V(C,C) representing the C-C bonds. In the case of ethene, the double bond is represented by two equivalent basins located symmetrically against the plane containing all atoms, having a collective electron population as large as 3.33e.

The calculated ellipticity at the bcp reflects the local symmetry of the electron density distribution, and can be a useful tool to characterize a C-C bond in terms of π and σ character.[8,26] The ellipticity of the CH_3-CH_3 bond (ε = 0), reflecting the local axial symmetry of the electron density distribution, is as expected for a single σ-bond. The ellipticity increases considerably for the bonds in C_6H_6 (ε = 0.20) and CH_2=CH_2 (ε = 0.33), which indicates an increasing contribution of π-electrons to the bonding density, just as expected for delocalized and double bonds.

Parameters calculated for bonds in C_{70} adopt values in the range typical for strong covalent bonds, with large values for V(C,C) and ρ, and large negative values for Δρ and H. As expected, C_a-C_b and C_c-C_c bonds to a large extent share many features with a standard double bond, as documented above for CH_2=CH_2. Of all eight bond types, these two have the shortest bond length, the largest electron density at the bcp, the largest V(C,C) bond population and

the largest ellipticity. The numerical values of most parameters, however, adopt values in a range between those typical of a pure double and pure delocalized bond. Contrary to CH_2=CH_2, the bond is represented by a single V(C,C) basin. We attribute this phenomenon to the fact that the surface of the fullerene is curved, which breaks the planar symmetry typical for CH_2=CH_2, and the electron pairs formed by the π-electron density tend to occupy the outer, rather than the inner, space of C_{70}.

Parameters calculated for the remaining six bond types adopt values between those typical for a single bond and for a delocalized bond, which clearly indicate contributions from the π-electron density. The numbers seem to support the point expressed in the experimental paper by Heymann that [5,6] 'single' bonds have some contributions from π-electron density. Those which are closer to the apical part (C_a-C_a, C_b-C_c and also C_c-C_d) were expected to be have more 'single' bond character, whereas the C_d-C_d bond, which is close to the equatorial belt is more 'aromatic'.[1] For the first group of bonds, the calculated ellipticities at the bcp adopts the lowest value (0.14), the lowest bond population (2.42 – 2.43e) and the lowest value of the electron density at the bcp, c.a. 0.285 au. We suspect that all these bonds should exhibit similar chemical properties. The next group, consisting of C_d-C_d and C_d-C_e, have larger contribution from the π-electron density, which is reflected by a larger value of ε (0.18). These bonds also have larger values of V(C,C) basin populations (2.65e and 2.71e) and larger values of electron densities at the bcp (0.292 – 0.300 a.u.). We should remember, however, that contrary to C_d-C_d, the C_d-C_e bond lies at the fusion of two six-member rings, so properties of the bonds may differ. The remaining group of C_e-C_e bonds, also at the fusion of six-member rings, seem to be different from all other groups. The ellipticity is 0.14, which indicates small, but not negligible, contributions from the π-electron density, but the bond is longer and weaker (as suggested by the value of ρ = 0.271 a.u. at bcp) than C_a-C_a, C_b-C_c and C_c-C_d.

To sum up, two out of eight types of bonds in C_{70} share features typical of double bonds, whereas the remaining six other types of bonds are single bonds with contributions from π-electron density. These findings are in line with conclusions reported in experimental papers.

Bond properties in $C_{70}O_3$ and $C_{70}O$ isomer series.

The first step in the general mechanism for ozonolysis involves O_3 insertion to a C=C bond, *via* a 1,3 cycloaddition reaction. Formation of the resulting molozonide intermediate draws π-electron density from the C=C bond into the newly formed C-O bonds, leaving a single σ

bond between the underpinning carbon atoms.[5,6] The parameters calculated for the C-C bonds bridged by the O_3 unit in the $C_{70}O_3$ isomer series (**Table 2**) clearly indicate that these bonds have true single bond character. First of all, for all eight molozonide isomers the ellipticity drops to 0.04, which confirms local axial symmetry of the electron density distribution. Moreover, the range of calculated electron densities at the bcps (0.166 – 0.226 a.u) and energy densities at the bcps (-0.097 – -0.175 a.u.) are all consistent with values obtained for CH_3-CH_3. The electron populations of the V(C,C) basins are slightly larger than for a pure single bond, but they are still considerably smaller than the corresponding values obtained for CH_2=CH_2 and C_6H_6.

It is a similar story for the a,b-$C_{70}O$ and c,c-$C_{70}O$ epoxides (**Table S1**, Supplementary Materials), where the topology analysis shows that most parameters calculated for the underpinning C-C bonds are consistent with the picture of a single covalent bond. The only caveat is the strikingly large values obtained for the bond ellipticities, which is a consequence of the proximity of the C-O-C ring critical point (in a three-membered ring) to the C-C bond critical point, a phenomenon known for three-member rings such as cyclopropane.[26] Our calculations (**Table 1**) suggest that the chemical bonds in C_{70} do not resemble pure single or double bonds. Although contributions from the π-electron density to C_a-C_a, C_b-C_c, C_c-C_d, C_d-C_d, C_d-C_e and C_e-C_e 'single' bonds are not negligible (particularly in the case of C_d-C_d and C_d-C_e bonds), it seems that these bonds may not be able to serve as an active site for an electrophilic addition reaction. But if the formation of an adduct requires π electrons to form new bonds between the reactants, how can we then explain the fact that all eight isomers of $C_{70}O_3$ refer to stable structures on the potential energy surface?[2]

In **Figure 4** we present changes in calculated properties of selected C-C bonds upon formation of the c,c-$C_{70}O_3$ isomer (see also **Table S2**, Supplementary Materials). Apart from the C_c-C_c bond (to which the O_3 unit is attached) we also present data for the adjacent bonds (C_b-C_c and C_c-C_d), as well as those that are further afield (C_a-C_b, C_b-C_c', C_d-C_d and C_d-C_e, see **Scheme 1** for atom labeling).

As expected, the largest changes in bond parameters are present for the C_c-C_c bond which forms the five-membered ring with the O_3 moiety. The bond elongates by 0.241 Å and the electron population of the V(C,C) bond decreases by as much as 0.95e. It is accompanied by a decrease in the electron density at the bcp, along with changes in both H and Δρ, all of which indicate that the C_c-C_c bond becomes a bit less covalent. As discussed earlier, we also observe

a change in the ellipticity, from 0.21 in the bare fullerene to 0.04 in the molozonide. To sum up, upon formation of the molozonide, the C_c-C_c bond loses its partial double bond character, and becomes a weaker, single bond with almost axial symmetry of the electron density distribution.

The presence of the O_3 unit bridging the C_c-C_c bond also influences the properties of the adjacent bonds (C_b-C_c and C_c-C_d), leading to a decrease in the electron population of these bonds by *ca*. 0.30e, and a lowering of the bond ellipticities. Interestingly, the electron populations of the V(C,C) basins representing the bonds that lie further afield increases slightly, by up to 0.18e (black squares in **Figure 4**), which is accompanied by a slight increase in the bond ellipticities and the bonds shorten (*i.e.* these bonds have slightly more π-character).

The data plotted in **Figure S1** and collated in **Table S3** (Supplementary Materials) indicate that the bonding situation in isomer a,b-$C_{70}O_3$ in the vicinity of the ozone bridge is quantitatively the same as that described above for the c,c isomer.

A slightly different situation is observed for the isomer e,e-$C_{70}O_3$ (**Figure 5**, **Table S4** Supplementary Materials), where the presence of the O_3 unit leads to a decrease in the electron population by some 0.5e, not only for the C_e-C_e bond but also for all four adjacent C_d-C_e bonds. Interestingly, it seems that all five bonds lose contributions from the π-electron density, which is reflected in a drop in ε to a value of 0.05 or below. The bonds become slightly longer, which is also accompanied by a decrease in the electron density at the bcp, along with an increase in Δρ and H. As a result, in e,e-$C_{70}O_3$ it is not only the C_e-C_e bond, but also all adjacent C_d-C_e bonds that adopt single bond characteristics.

To sum up, in a,b-$C_{70}O_3$, c,c-$C_{70}O_3$ and e,e-$C_{70}O_3$ the formation of the ozone bridge over the C-C bond leads to observable changes in the properties of the chemical bonds in the vicinity of the O_3 unit. The C-C bond, along with the adjacent bonds, become single bonds whereas electron population of the V(C,C) basins representing the bonds further afield slightly increases. This mechanism thus explains how adducts can form with bonds other than the 'double' C_a-C_b and C_c-C_c bonds: if the contribution of the π-electrons from the underlying bond itself is small, then all four adjacent bonds can effectively contribute their π-electrons to form the new adduct bonds.

To check how far the redistribution of the electron density can propagate through the net of carbon – carbon bonds, we plotted the changes in V(C,C) populations for all 105 bonds present in c,c-$C_{70}O_3$ (**Figure 6**), a,b-$C_{70}O_3$ (**Figure S2**) and e,e-$C_{70}O_3$ (**Figure 7**) and labelled the cases for which the change in the electron population upon molozonide formation is larger than 0.1e. The data plotted in the figures indicate that redistribution of the electron density can be observed up to three bonds from the ozone unit. Interestingly, in the case of e,e-$C_{70}O_3$ the changes in the basin populations in the vicinity of the O_3 moiety are not as large as for isomers a,b and c,c, but they decay at a slower rate with the distance from the ozone ring and at a distance of three bonds the changes exceed 0.2e (**Figure 7**).

The formation of a molozonide structure can lead to an increase or a decrease in the electron population of the bonds in the carbon cage. Typically, the population of the adjacent bonds and those located three bonds away from the O_3 unit decrease, whereas populations in bonds that are two bonds from the bridge usually increase. This leads to an important conclusion regarding any functionalization strategy for C_{70}: the properties of the surface of the fullerene derivatives may be significantly different from those of the pristine fullerene.

The changes in bond properties due to c,c-$C_{70}O$ oxide formation (**Figure S3** Supplementary Materials) seem to be more localized that those observed for the corresponding molozonide (**Figure 4**). But while the decrease in the C_c-C_c bond population is large (1.27e, vs. 0.95 for the molozonide), the changes in the properties of the adjacent bonds are small, and all other bonds further afield seem to be almost unperturbed. A very similar bonding situation emerges for the epoxide a,b-$C_{70}O$ (**Figure S4** Supplementary Materials).

A qualitatively different bonding situation is apparent for the epoxide e,e-$C_{70}O$, as illustrated in **Figure S5** (Supplementary Materials). According to our computational results, this isomer has an open, oxidoannulene, structure. The C_e…C_e distance is ca. 0.78 Å longer than in bare C_{70} and we did not find a bond critical point or a valence ELI-D basin between these atoms. The cleavage of the C_e-C_e bond upon formation of the oxide leads to a slight increase in the population of V(C,C) basins representing the adjacent d,e bonds by some 0.24e, which is accompanied by a slight increase in the bond ellipticities. The properties of the subsequent bonds are almost unchanged. This result is in line with the point expressed in the experimental paper by Hey et al,[1] that the processes on the C_{70} surface leading to the cleavage of a 'single' bond do not considerably effect the 70 electrons contributing to π-electron density.

Figures S6, S7, S8 (Supplementary Materials) illustrate how changes in electronic structure upon oxide formation propagate along the net of C-C bonds. As for the molozonides, we have plotted the changes in the electron population for all 105 C-C bonds in c,c-$C_{70}O$, ab-$C_{70}O$, and 104 bonds e,e-$C_{70}O$, in comparison to bare fullerene. The changes in the V(C,C) basin populations are large and localized close to the ozone ring and they decay at a faster rate with the distance from the ozone ring than those for the ozonide molecules.

Relative stability of the ozone isomers.

In the previous paragraphs we have discussed the bonding situation in C_{70} and the role of the redistribution of electron density in the formation of isomers of $C_{70}O_3$. Now we go a step further and attempt to explain the relative stabilities of the ozonide series (**Table S5**) in terms of the bond properties in C_{70} and $C_{70}O_3$. We define the relative stability of molozonides as the energy of relevant structures on the potential energy surface expressed in relation to the most stable isomer, a,b-$C_{70}O_3$. The fact that a,b-$C_{70}O_3$ and c,c-$C_{70}O_3$, two experimentally known ozonides, are the most stable isomers seems easy to justify. As the formation of moloozonides typically proceeds through the addition of O_3 to a double (multiple) C-C bond, it should be expected that bonds sharing the character of a double bond should lead to the most stable products. If we assume that the electron population of the V(C,C) basin reflects the character of the bond, then we might expect the relative energy of a molozonide to decrease with the increasing population of the V(C,C) bond basins in the parent C_{70}.

Moreover, as demonstrated for e,e-$C_{70}O_3$, ozone addition to bonds other than C_a-C_b and C_c-C_c extensively utilizes the π-electron density from adjacent bonds and influences V(C,C) basin populations of other bonds in the fullerene. Thus it might be suspected that larger perturbations in the bond populations lead to products that are higher in energy.

To verify these hypotheses we have plotted the relative stabilities of the x,y-$C_{70}O_3$ isomers versus V(C_x,C_y) bond population in a parent C_{70} molecule (**Figure 8 - upper panel**) and versus total perturbation of the bonding density (**Figure 8 - lower panel, Table S5**). The latter parameter is calculated as the sum of perturbations over all 105 C-C bonds in a $C_{70}O_3$ isomer. A perturbation for a given bond is calculated as an absolute value of the difference of the V(C,C) basin population in C_{70} and the bond population in $C_{70}O_3$, i.e. $|V_{fullerene}(C,C) - V_{molozonide}(C,C)|$.

Figure 8 – upper panel shows the isomer stability plotted versus the population of the $V(C_x,C_y)$ basin in the parent molecule. Plotting a linear fit for the set of seven isomers (e,e-$C_{70}O_3$ excluded) yields R^2=0.796, and R^2=0.857 for the set of six isomers (e,e-$C_{70}O_3$ and d,d-$C_{70}O_3$ excluded) indicating that a rough correlation is present. The value of the electron populations of basins representing bonds in C_{70} can be useful in identifying bonds that are likely to have dominant double bond character, and therefore may serve as a preferred site for an addition reaction. However, this factor cannot be used to explain quantitative differences in the stabilities of adducts formed over C-C bonds that have only minor contributions from the π-electron density network.

Apart from the e,e-$C_{70}O_3$, isomer stabilities appear to correlate better with bond population perturbations (**Figure 8 – lower panel**). A linear fit for the dependence between the C_{70} bond population perturbation and the stability calculated for seven isomers has R^2=0.877 (see the trend line in **Figure 8**). The fit is much better (R^2=0.969) for the set of six isomers, where d,d-$C_{70}O_3$ is also excluded. We cannot provide an explanation that accounts for the fact that the e,e-$C_{70}O_3$ isomer does not match the discussed stability trend. It is worth noticing, however, that fullerenes are stiff structures, where local structural modifications related to bond formation or decomposition may lead to strain being exerted on the whole molecule. The C_e-C_e bond in C_{70} is the longest one, and molozonide formation leads to further bond length elongation by 0.263 Å, whereas other bonds in the cage are elongated by 0.201 – 0.238Å. As a consequence, the electron density at the bond critical point for C_e-C_e has the lowest value both in the fullerene and in the molozonide structure.

It is not surprising that the total perturbation of the bonding density in the product of ozone addition correlates better with the relative stability of isomers than the electron populations of V(C,C) basins in the parent C_{70}, as the latter parameter does not take into account an influence of the identity of the second reactant. Moreover, contrary to the V(C,C) basin population, which reflects some local properties of the fullerene surface, the total perturbation of the bonding density considers the response of the whole fullerene structure with respect to surface functionalization.*Bond evolution in the course of the ozone ring opening reaction.*

The spontaneous ozone ring opening reaction observed in the course of an MD run for e,e-$C_{70}O_3$ is triggered by the dissociation of the underpinning C-C bond. It is immediately followed by the dissociation of one of the O-O bonds.[2] The mechanism of the reaction is the same also for a molozonide doped with a noble gas atom[3] or a light molecule.[4] A minimum

energy path plotted in **Figure 9 - upper panel** indicates a small energy barrier for the ring opening reaction related mainly to the cleavage of the C-C bond (marked by TS – transition state – on the figure). In the local (molozonide) minimum we have a C-C covalent bond represented by a disynaptic basin populated with 1.88.e (**Figure 9 - lower panel, Figure 10**). At the transition state the basin splits into two monosynaptic basins populated collectively by 1.54e, which indicates the point at which the C-C covalent bond breaks. The basins quickly disappear with further elongation of the C-C distance. The electron density at the bcp is relatively small for the equilibrium structure, which is in line with the low energy barrier observed for the bond dissociation reaction. The value of the electron density decreases with bond elongation, but even after crossing the transition state the critical point related to the C…C interaction does not completely disappear, but the value of the electron density at this point is very small.

The O-O bond is represented by two monosynaptic basins with a total population of only 0.54e. The basins immediately disappear when the bond starts to elongate. Low electron population of the basins representing the bond might be surprising when collated to a large value of the electron density at the bond critical point (0.299 a.u at equilibrium). These results, however, are consistent with the properties of O-O bond in H_2O_2, discussed extensively in earlier papers by some of us.[27,28] The bond in H_2O_2 is classified as protocovalent, with a large value of the electron density at the bcp (0.273 a.u) and two monosynaptic basins populated together with 0.56e. As depicted in **Figure 9**, the dissociation of the O-O bond is almost barrierless.

The ozone ring opening reaction in c,c-$C_{70}O_3$ (**Figure 11**) and a,b-$C_{70}O_3$ (**Figure S9** Supplementary Materials) have larger energy barriers, which is consistent with the shorter C-C bond in the equilibrium structures (1.59 Å and 1.62 Å, respectively). Minimum energy paths compared to the relevant bond lengths plotted against the reaction coordinate now indicate the simultaneous dissociation of the C-C and O-O bonds. The population of the V(C,C) basin in the equilibrium structure of c,c-$C_{70}O_3$ is 2.00e and decreases with bond elongation up to the transition state where the basin splits into two monosynaptic basins with a total population of 1.22e (**Figure 11**). With further elongation one of the basins quickly disappears, while the second one gets negligibly small. Although the V(C,C) basin splits at the TS, which indicates the decomposition of the covalent bond, the critical point of the energy density, along with a small value for the electron density, can still be detected in the ring open product. The electron density at the O-O bcp decreases from 0.287 a.u. at the

reactant (R(O-O) = 1.48 Å) to 0.05 a.u. in the product (R(O-O) = 2.66 Å). In the closed molozonide structure the bond can be classified as protocovalent, and is represented by two monosynaptic basins with a total population of 0.52e which quickly disappears after a small elongation of the O-O bond. A similar picture of the ozone ring opening reaction can be observed for the a,b isomer, as depicted in **Figure S9** (Supplementary Materials).

Conclusions:

Theoretical methods based on a quantum chemical topology approach revealed that chemical bonds in C_{70} do not have typical properties expected for the limiting cases of single or double bonds, as parameters calculated for all C_x-C_y bonds usually adopt intermediate values. C_c-C_c and C_a-C_b bonds have dominant characters expected of a double bond, whereas the remaining six bonds, (C_a-C_a, C_b-C_c, C_c-C_d, C_d-C_d, C_d-C_e and C_e-C_e) can be considered more as single bonds with some contributions from the π-electron density network. These findings are in line with suggestions in earlier papers. Depending on the chemical processes considered these bonds may exhibit chemical reactivity expected for a single or a double bond. In the first case, the formation of a product leads to the cleavage of a C-C bond, as is observed upon oxidoannuene formation. Alternatively, when the bond acts as a double bond, the formation of a product retains the C-C bond, as in C_{70} molozonides. Numerical values of parameters characterizing bond properties indicate that among the six bonds with predominant single bond character, C_d-C_d and C_d-C_e have the largest contribution of the π-electron density whereas the C_e-C_e bond has the lowest. The group of C_a-C_a, C_b-C_c and C_c-C_d bonds should have similar chemical properties, as indicated by values of calculated parameters.

The fact that all eight bond types, two ‘double’ and six ‘single’, can be active sites in the addition of O_3 can be explained by the fact that it is not only contributions from the π-electron density from a given bond that is engaged in the formation of new C-O bonds, but that π-electron density from all four adjacent bonds contribute effectively to the process. As a result both the underpinning C-C bond and the adjacent bonds become single C-C bonds in the $C_{70}O_3$ product.

The changes in the electron density in C_{70} upon ozonide formation can propagate through the net of C-C bonds and at a distance of three bonds away from the ozone ring can still be as large as 0.1e. This observation may be important for a functionalization strategy of C_{70} as it indicates that chemical properties of the pristine fullerene can be different from the properties of its derivatives.

The calculated relative stabilities of most ozonide isomers correlates well with the total perturbation of the bonding density in the molecule – the smallest perturbation is observed in the most stable isomers. However, topological analyses do not provide clear explanations as to why e,e-$C_{70}O_3$, the least stable isomer, is so high in the energy scale compared to the other isomers.

Finally, the evolution of the ELI-D basin representing the C-C bond involved in the ozone ring opening reaction on the fullerene surface correlates well with the calculated minimum energy path. The population of the disynaptic basin V(C,C) decreases with the elongation of the bond. At the transition state the basin splits into two monosynaptic basins with further decreases in the bonding electron density. This indicates that the covalent C-C bond breaks when the system crosses the energy barrier. The O-O bond in the ozone ring has at equilibrium a large value of the electron density at the bond critical point but is represented by two monosynaptic basins populated with a small electron density. The bond resembles the properties of the single O-O bond in H_2O_2 and can be classified as protocovalent. It easily dissociates as the monosynaptic basins quickly disappear with small perturbation of the equilibrium distance.

5 Acknowledgments

Andrzej Bil would like to thank the Ministry of Science and Higher Education, Republic of Poland, for supporting this work under the grant no. N N204 280738 and to the Scientific Exchange Programme between the New Member States of the EU and Switzerland for financial support. Electron localizability indicator was plotted with the UCSF Chimera package.[29]

References:

(1) Heymann, D.; Bachilo, S.M.; Weisman, R.B.; *J. Am. Chem. Soc.* **2002**, 124, 6317**.**

(2) Bil, A.; Latajka, Z.; Morrison, C.; *J. Phys. Chem. A* **2009**, 113, 9891.

(3) Bil, A.; Morrison, C.; *J. Phys. Chem. A* **2012**, 116, 3413.

(4) Bil, A.; Latajka, Z.; Morrison, C.; *Chem. Phys.* dx.doi.org/10.1016/j.chemphys.2013.10.011

(5) Criegee, R. *Angew. Chem. Int. Ed. Engl*. **1975**, 87, 745.

(6) Geletneky, C.; Berger, S. *Eur. J. Org. Chem.* **1998**, 8, 1625.

(7) Meier, S. M.; Wang G.-W.; Haddon R. C.; Pratt Brock C.; Lloyd M. A.; Selegue J. P. *J. Am. Chem. Soc.*, **1998**, 120, 2337.

(8) Bader, R.F.W. Atoms in Molecules: A Quantum Theory, Oxford University Press, Oxford **1990.**

(9) Kohout, M.; Pernal, K; Wagner, F.R.; Grin, Y. *Theor. Chem. Acc.* **2004**, 112, 453. (10) Kohout, M.: *Int. J. Quantum Chem.* **2004**, 97, 651.

(11) Kohout, M. *Faraday Discuss.* **2007**, 135, 43.

(12) Krokidis, X.; Noury, S.; Silvi, B. *J. Phys. Chem.* **1997**, 101, 7227.

(13) Becke, A. *Phys. Rev A* **1988**, 38 , 3098.

(14) Lee, C.; Yang, W.; Parr, R. *Phys Rev B* **1988**, 37, 785.

(15) Lippert, G; Hutter, J.; Parinello, M.; *Mol. Phys.* **1997**, 92, 477.

(16) Vande Vondele, J.; Krack, M; Mohamed, F; Parrinello, M; Chassaing, T; Hutter, J. *Comp. Phys. Commun.* **2005**, 167,103.

(17) The CP2K developers group, http://cp2k.org/

(18) Grimme, S.; Antony, J.; Ehrlich, S.; Krieg, H. *J. Chem. Phys.* **2010**, 132, 154104.

(19) Goedecker, S; Teter, M; Hutter, J. *Phys. Rev. B* **1996**, 54, 1703.

(20) Henkelman, G; Jonsson, H. *J. Chem. Phys*. **2000**, 113, 9978.

(21) Becke, A. D.; Edgecombe K. E. *J.Chem.Phys.* **1990**, 92, 5397.

(22) Silvi, B.; Savin A. *Nature* **1994**, 371, 683.

(23) A. Schäfer, A.; Huber C.; Ahlrichs R. *J. Chem. Phys.* **1994**, 100, 5829.

(24) TURBOMOLE V6.4 2012, a development of University of Karlsruhe and

Forschungszentrum Karlsruhe GmbH, 1989-2007, TURBOMOLE GmbH, since 2007; available from www.turbomole.com

(25) M. Kohout, DGrid, version 4.6, Radebeul, 2011

(26) Popelier, P. Atoms in Molecules. An Introduction. Prentice Hall, **2000**.

(27) Bil, A.; Latajka Z. *Chem. Phys.* **2004**, 303, 43.

(28) Bil, A.; Latajka Z. *Chem. Phys.* **2004**, 305, 243.

(29) UCSF Chimera - a visualization system for exploratory research and analysis. Pettersen, E.F.; Goddard, T.D.; Huang, C.C.; Couch, G.S.; Greenblatt, D.M.; Meng, E.C.; Ferrin, T.E. *J. Comput. Chem.* **2004**, 25, 1605.

Table 1 Calculated properties of carbon – carbon bonds in C_{70}, ethane, ethene and benzene: R - equilibrium bond distance, V(C,C) - electron population of a valence ELI-D basin representing a bond, ρ – electron density at a bond critical point, Δρ – Laplacian of electron density at the bcp; ε – ellipticity of the electron density at the bcp, H – energy density at the bcp.

	R/ Å	V(C,C)	ρ/a.u.	Δρ/a.u.	ε	H/a.u.
C_a-C_a	1.45	2.43	0.283	-0.749	0.14	-0.269
C_a-C_b	1.39	2.95	0.313	-0.878	0.21	-0.323

C_b-C_c	1.45	2.42	0.284	-0.758	0.14	-0.272
C_c-C_c	1.38	2.95	0.318	-0.904	0.21	-0.333
C_c-C_d	1.45	2.42	0.285	-0.763	0.14	-0.273
C_d-C_d	1.43	2.65	0.292	-0.778	0.18	-0.285
C_d-C_e	1.42	2.71	0.300	-0.829	0.18	-0.299
C_e-C_e	1.47	2.45	0.271	-0.694	0.14	-0.247
ethane	1.55	1.78	0.230	-0.542	0	-0.186
benzene	1.42	2.74	0.300	-0.824	0.20	-0.298
ethene	1.36	3.33*	0.332	-0.724	0.33	-0.362

*In $H_2C=CH_2$ the double bond is represented by two equivalent basins located symmetrically above and below the symmetry plane established by the position of all atoms.

Table 2 Calculated properties of the carbon – carbon bonds bridged by O_3 in the $C_{70}O_3$ molozonides isomer series. R - equilibrium bond distance, V(C,C) - electron population of a valence ELI-D basin representing a bond, ρ – electron density at a bcp, Δρ – Laplacian of the electron density at a bcp, ε – ellipticity of the electron density at a bcp, H – energy density at a bcp.

	R/Å	V(C,C)	ρ/a.u.	Δρ/a.u.	ε	H/a.u.
C_a-C_a	1.65	1.97	0.201	-0.393	0.04	-0.141

C_a-C_b	1.62	1.99	0.214	-0.452	0.04	-0.159
C_b-C_c	1.66	1.96	0.190	-0.381	0.03	-0.138
C_c-C_c	1.59	2.00	0.226	-0.506	0.04	-0.175
C_c-C_d	1.63	1.99	0.209	-0.430	0.04	-0.152
C_d-C_d	1.67	1.96	0.194	-0.357	0.03	-0.131
C_d-C_e	1.63	2.01	0.207	-0.424	0.03	-0.148
C_e-C_e	1.73	1.88	0.166	-0.243	0.02	-0.097

Figure 1 The carbon atom environments in C_{70}

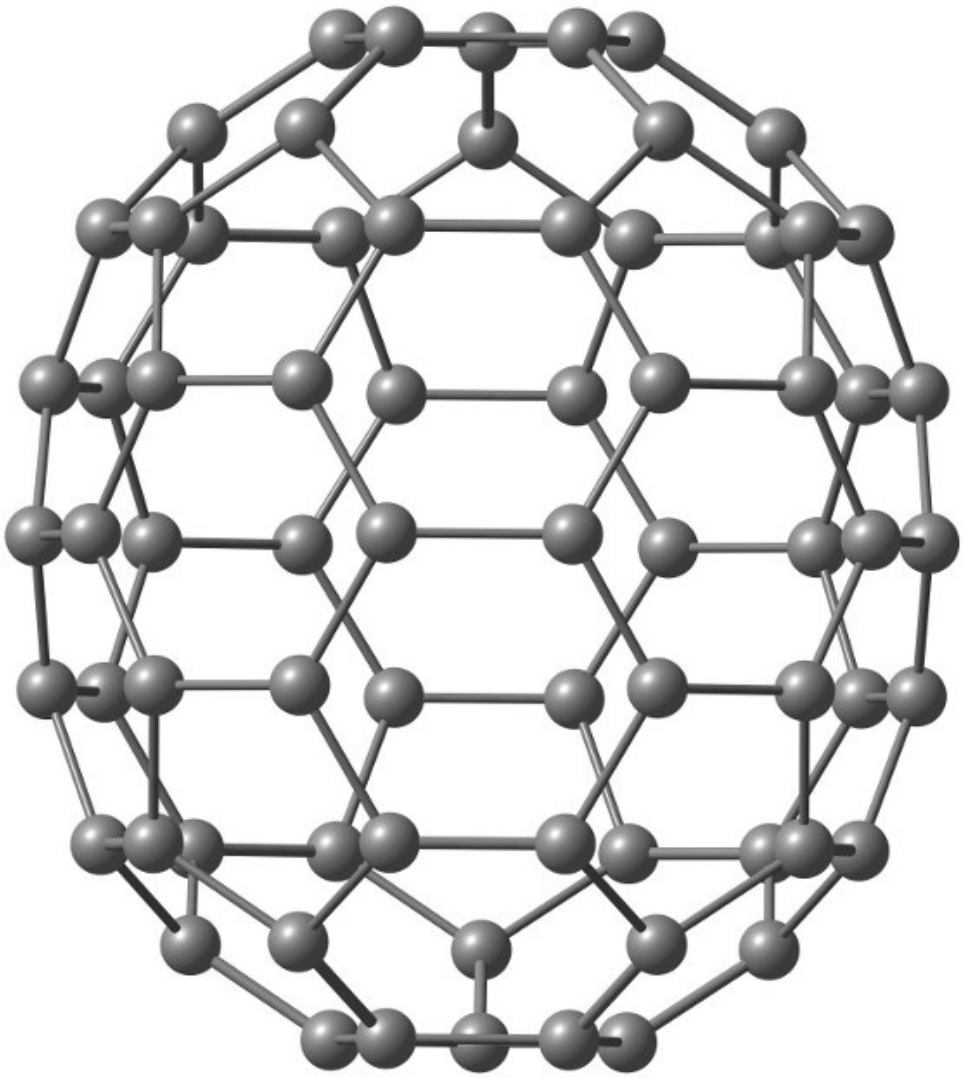
a
b
c
d
e
d
c
b
a

Figure 2 Relevant structural motifs typical for (1) molozonide, (2) the product of the molozonide ring opening reaction,(3) epoxide and (4) $C_{70}O$ oxidoannulene forms.

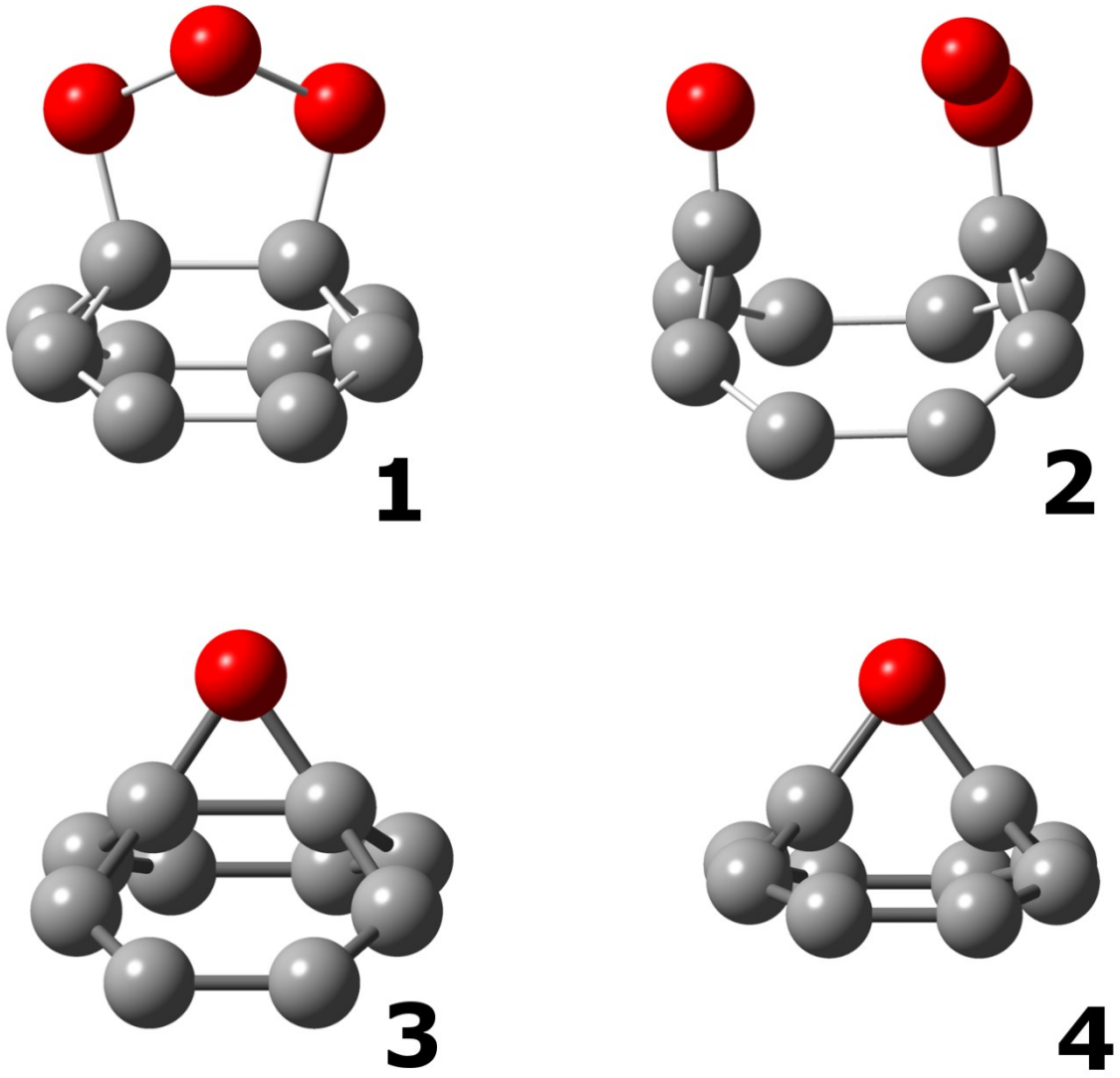

Figure 3 Localization domains of the electron localizability indicator (ELI-D) plotted for a,b-$C_{70}O_3$. Note the marked valence basins (V) representing electron lone pairs on the oxygen atoms (as a union of two monosynaptic basins), as well as C_a-C_b and in one of the C-O bonds.

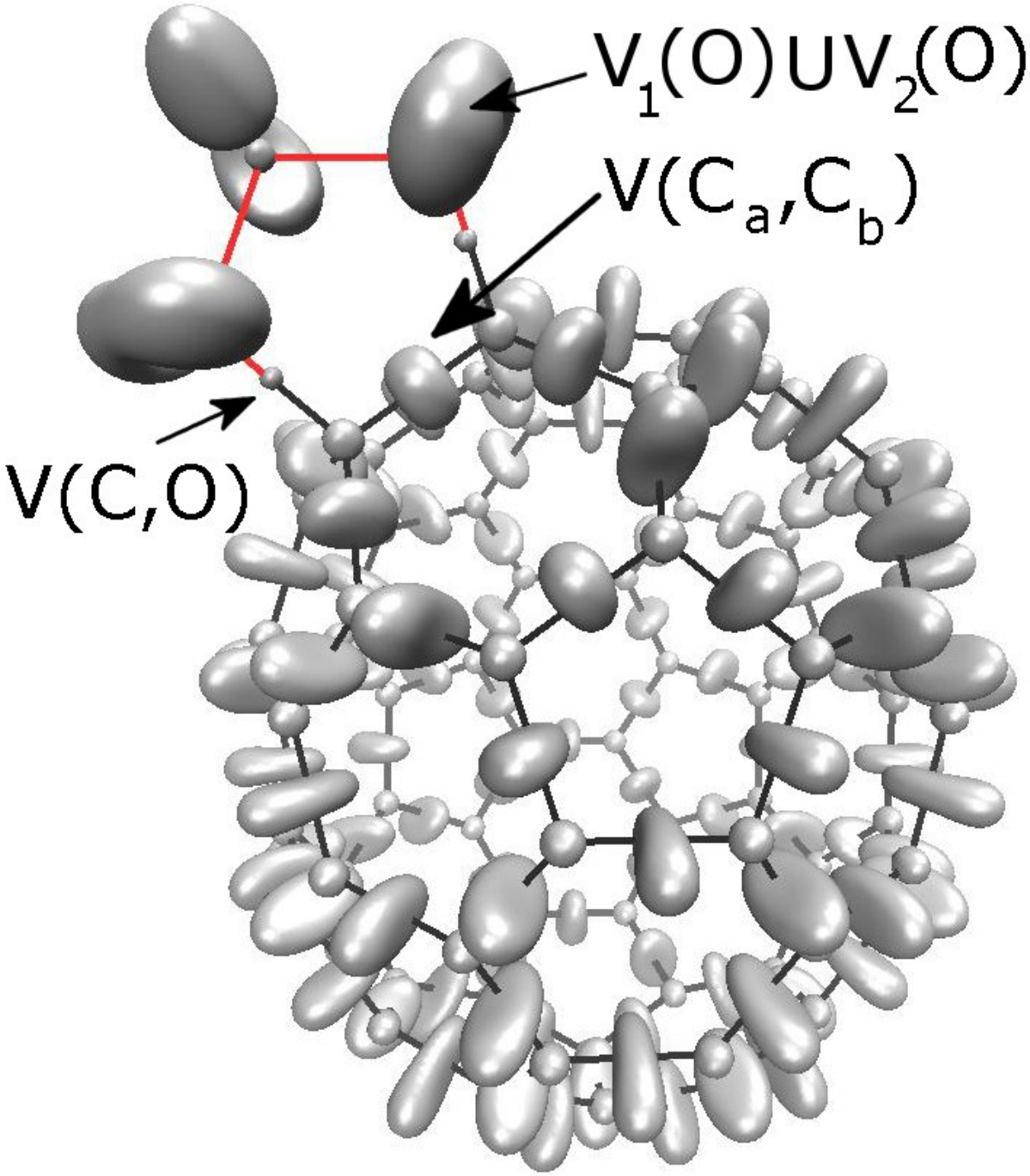

Figure 4 Changes in selected bond properties calculated for c,c-$C_{70}O_3$ vs. parent C_{70}. Differences in V(C,C) basins populations are plotted against the left axis, while differences in bond distances (R), electron densities at the bcp (ρ), the Laplacian of the electron densities (Δρ), ellipticities (ε) and energy densities (H) are plotted against the right axis.

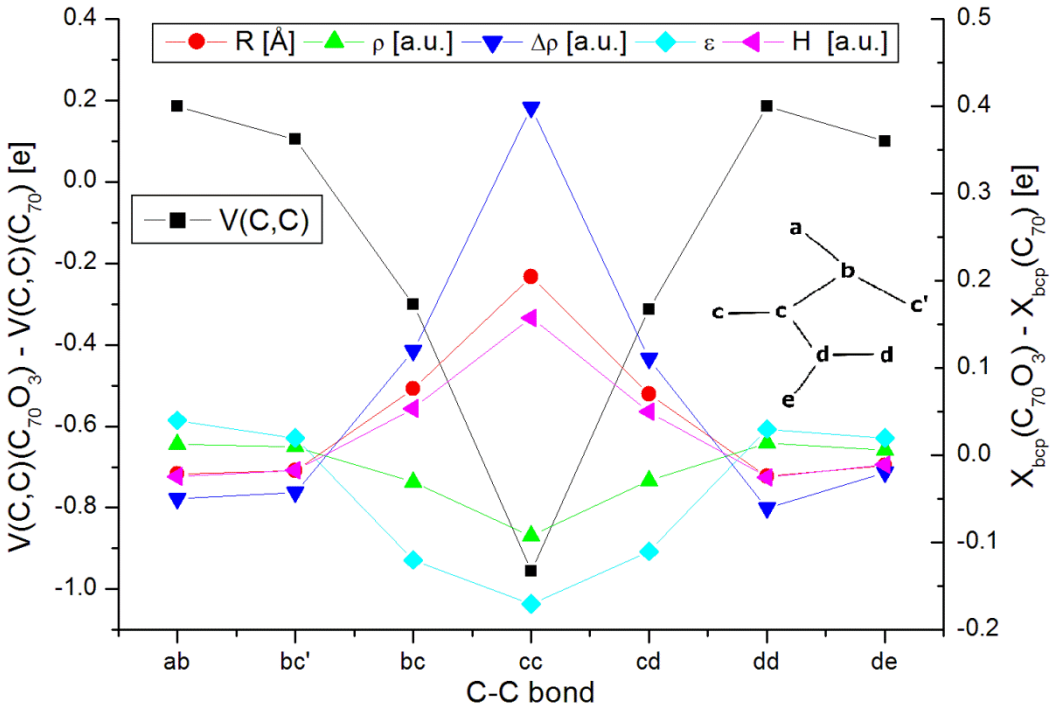

Figure 5 Changes in selected bond properties calculated for e,e-$C_{70}O_3$ vs. parent C_{70}. Differences in V(C,C) basins populations are plotted against the left axis, while differences in bond distances (R), electron densities at the bcp (ρ), the Laplacian of the electron densities (Δρ), ellipticities (ε) and energy densities (H) are plotted against the right axis.

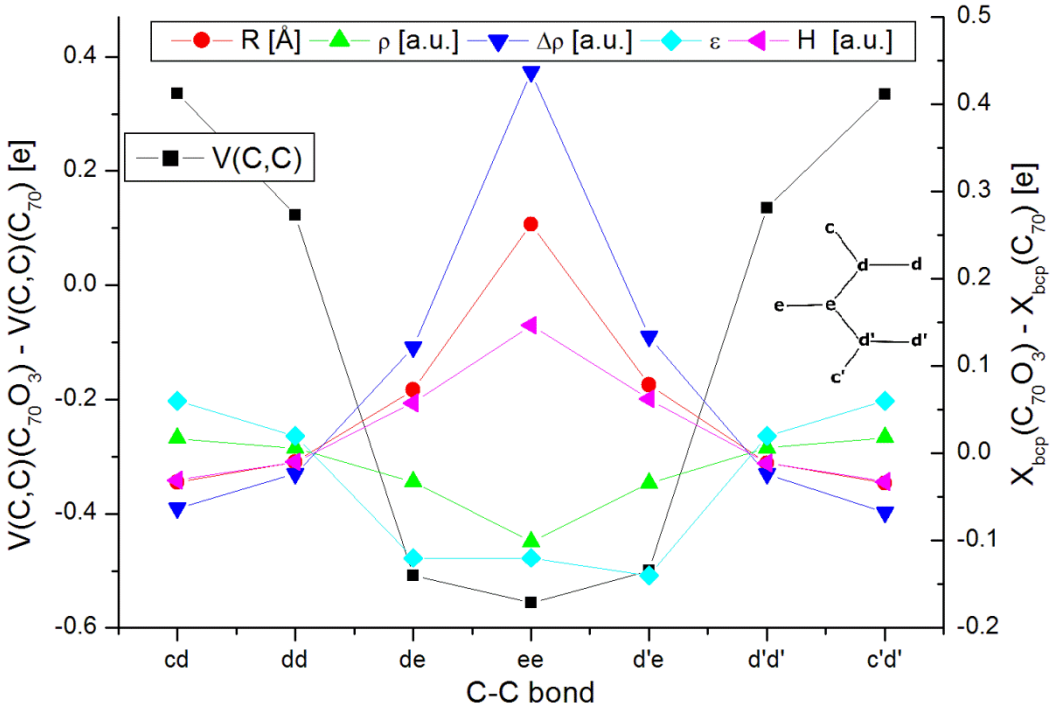

Figure 6 Changes in V(C,C) basins populations calculated for c,c-$C_{70}O_3$ vs. parent C_{70}. Upper panel represent bonds in the hemisphere proximal to the ozone ring (labelled 'up'), lower panel is plotted for the distal hemisphere (labelled 'down'). All bonds for which the changes are greater than 0.1e are shown, along with information on how far they are from the ozone ring (i.e. one two or three bonds from the ring).

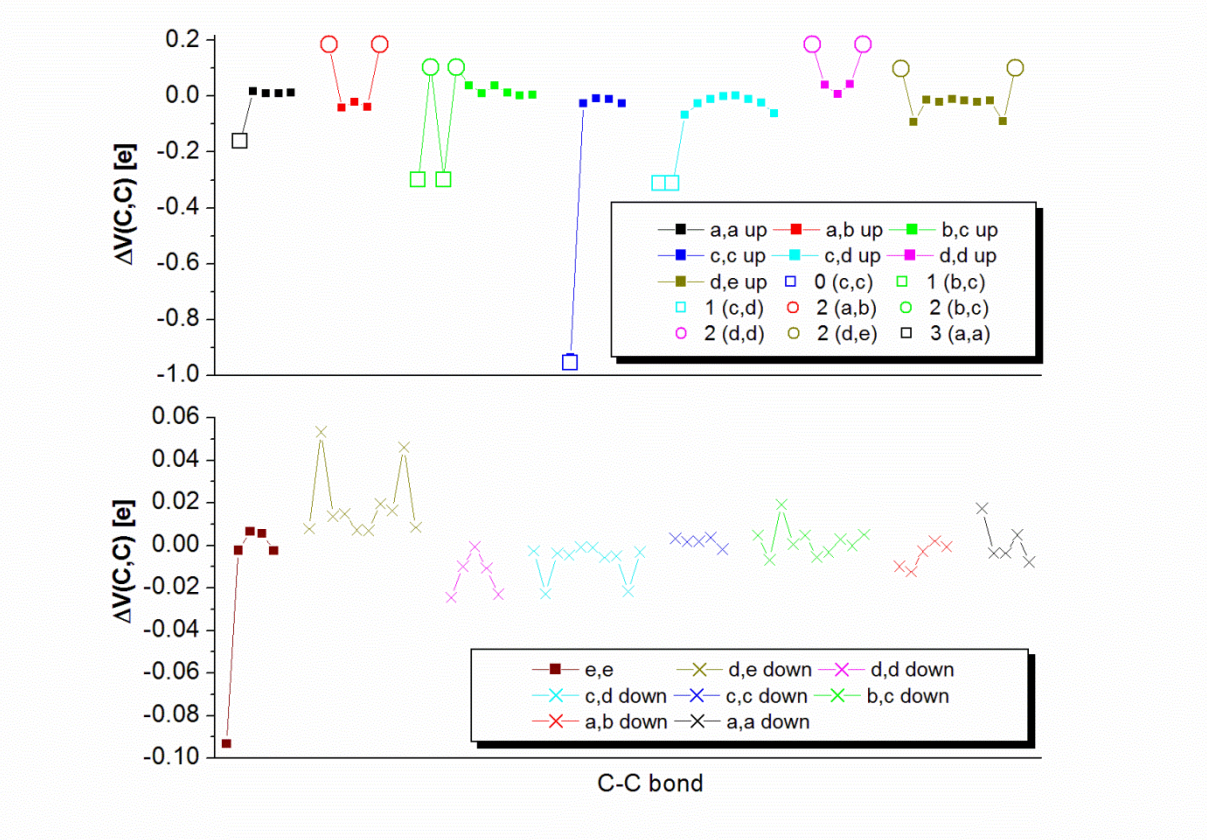

Figure 7 Changes in V(C,C) basins populations calculated for e,e-$C_{70}O_3$ vs. parent C_{70}. All bonds for which the changes are greater than 0.1e are shown, along with information on how far they are from the ozone ring (i.e. one two or three bonds from the ring).

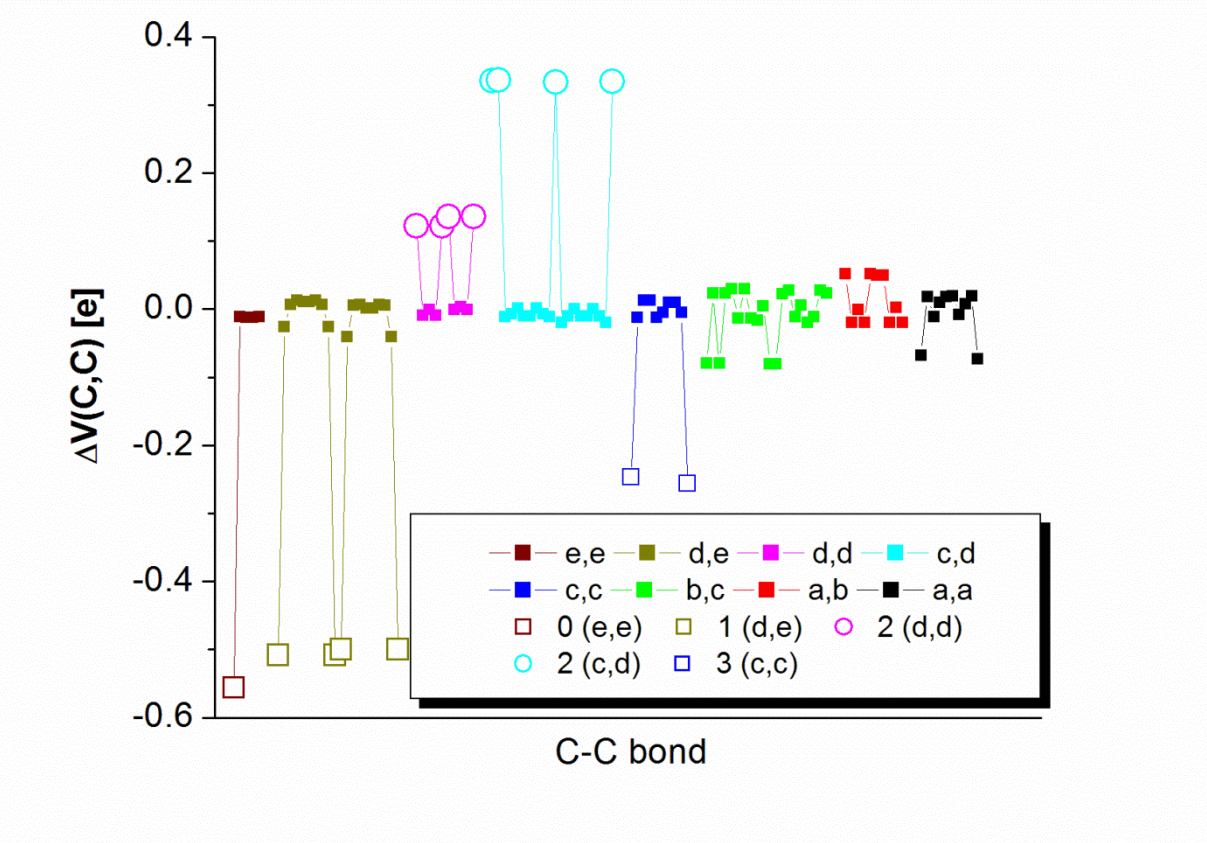

Figure 8 Stability of the molozonide isomers plotted against the C_x-C_y bond population in C_{70} (upper panel) and against the total perturbation of the population of V(C,C) basins (lower panel). A linear fit is made for the set of seven isomers (e,e-$C_{70}O_3$ excluded) with R^2=0.796 and 0.877 obtained for the upper and lower panel, respectively.

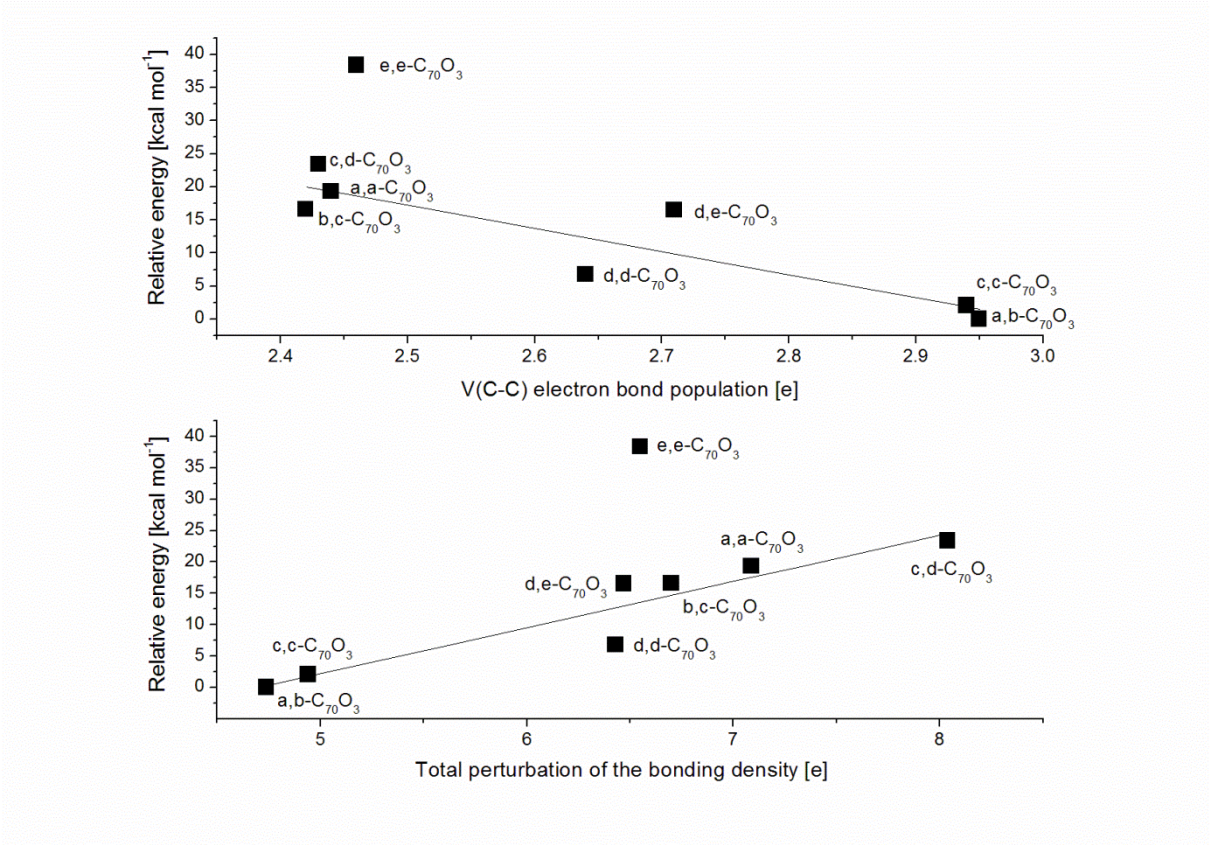

Figure 9 The minimum energy path, the evolution of the C-C and O-O bond distances (upper panel), and the evolution of the electron density at the (3,-1) critical points along with valence basin populations (lower panel) in the course of the ozone ring opening reaction for e,e-$C_{70}O_3$. We use $V(C_e)$/ $V(C_e')$ and V(O)/ V(O') to label monosynaptic basins belonging to two different carbon/oxygen atoms.

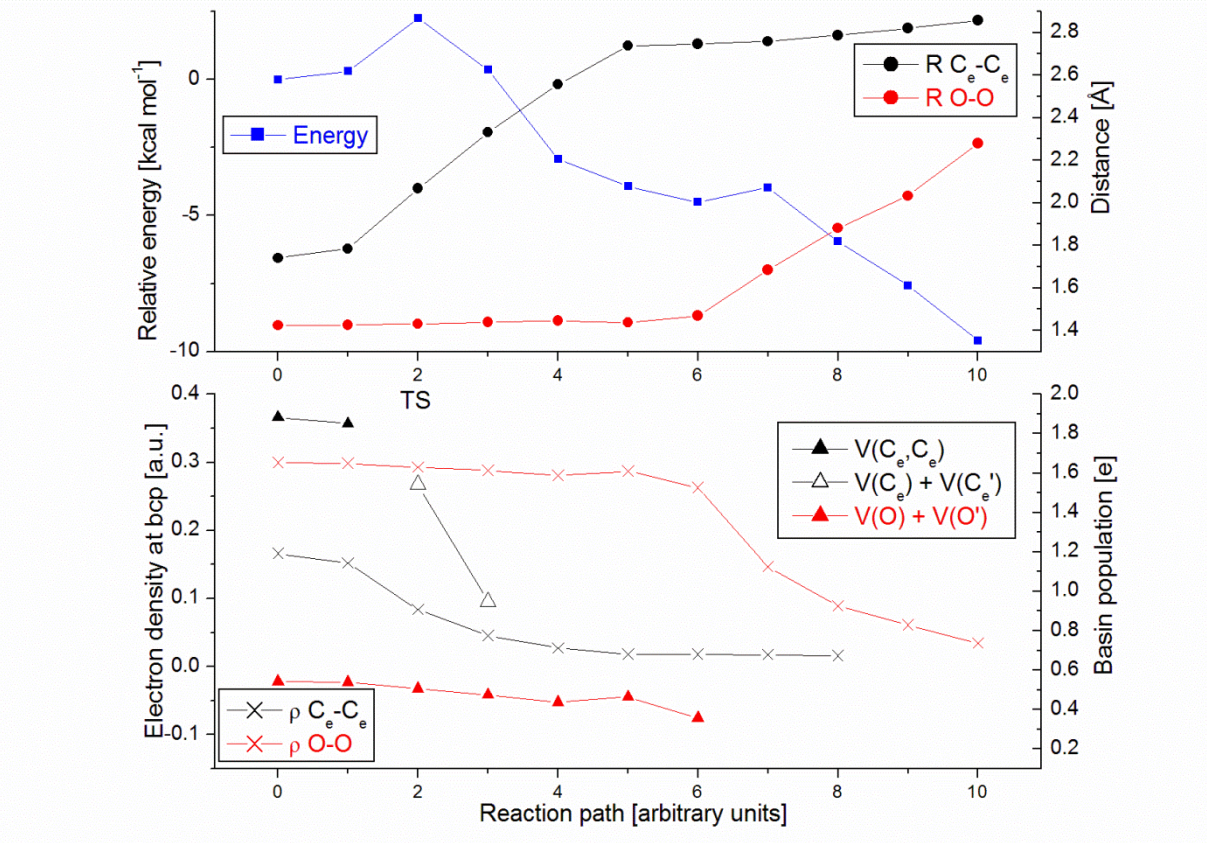

Figure 10 Evolution of the C-C bond in the course of the ozone ring opening reaction in e,e-$C_{70}O_3$. Localization domains of electron localizability indicator are plotted for the reactant (closed structure on the left,Y=1.48), transition state (in the middle,Y=1.42) and the product (open structure on the right,Y=1.47).

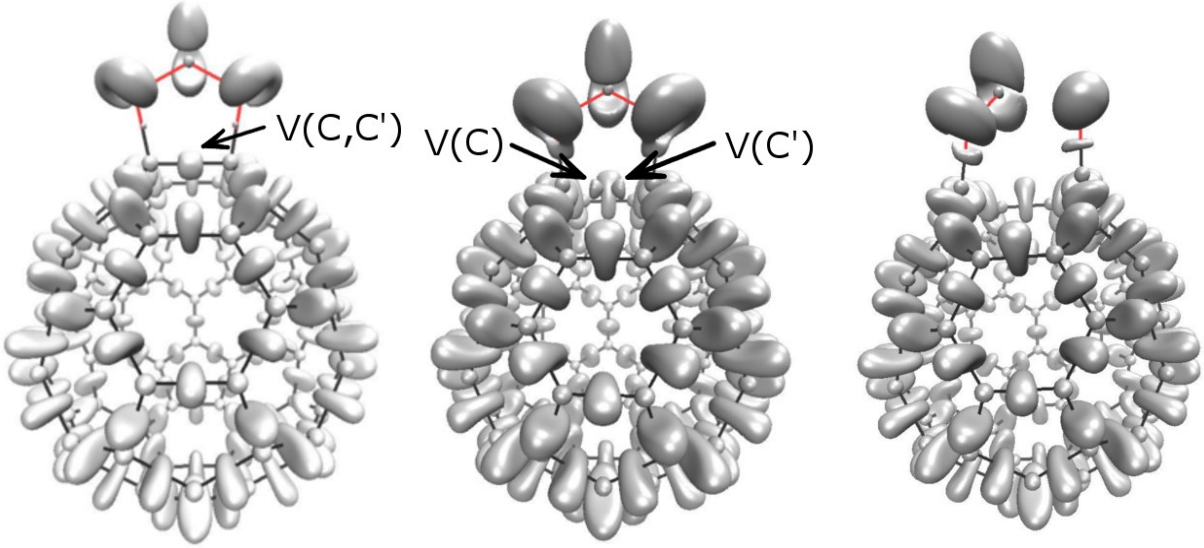

Figure 11 The minimum energy path, the evolution of the C-C and O-O bond distances (upper panel), and the evolution of the electron density at the (3,-1) critical points along with valence basinspopulations (lower panel) in the course of the ozone ring opening reaction for c,c-$C_{70}O_3$. We use V(C_c)/ V(C_c') and V(O)/ V(O') to label monosynaptic basins belonging to two different carbon/oxygen atoms.

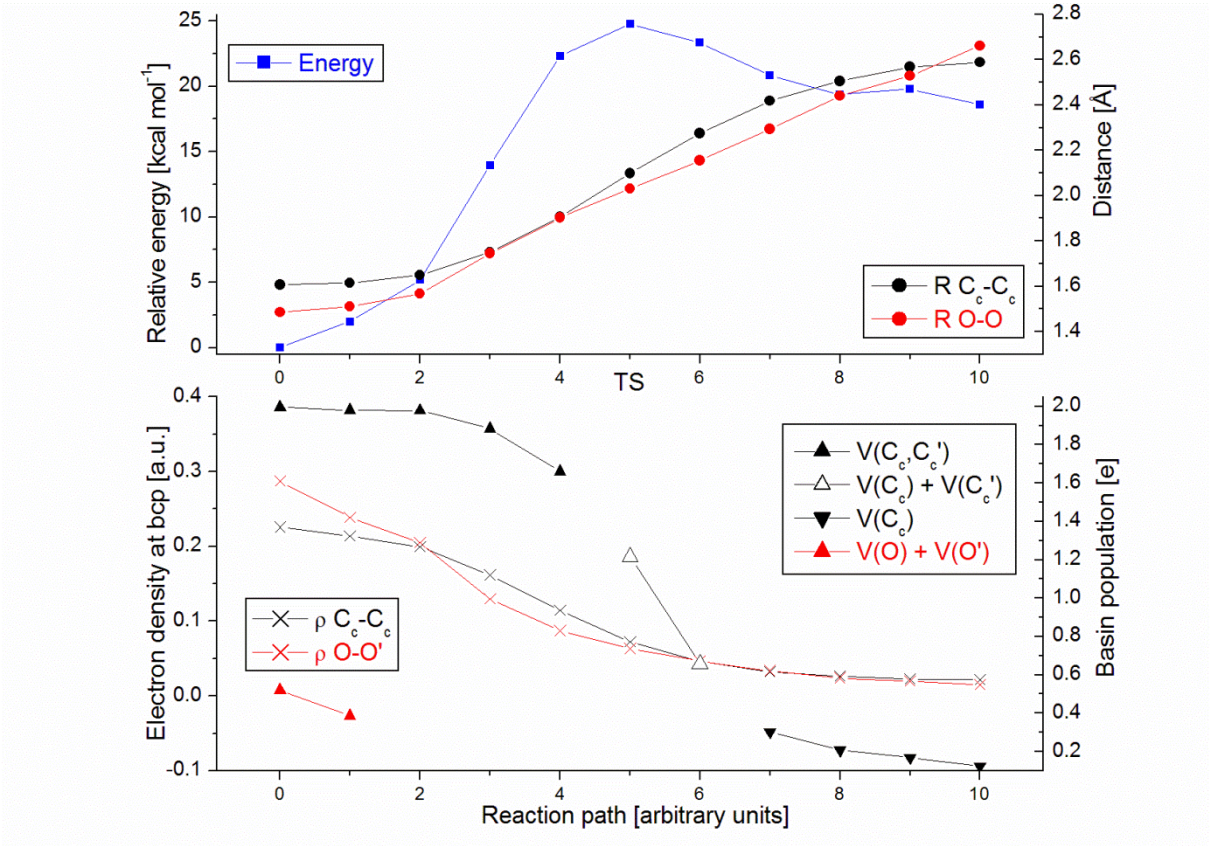

Figure TOC

Localization domains of the electron localizability indicator (Y=1.33) representing carbon-carbon bonds in C_{70}.

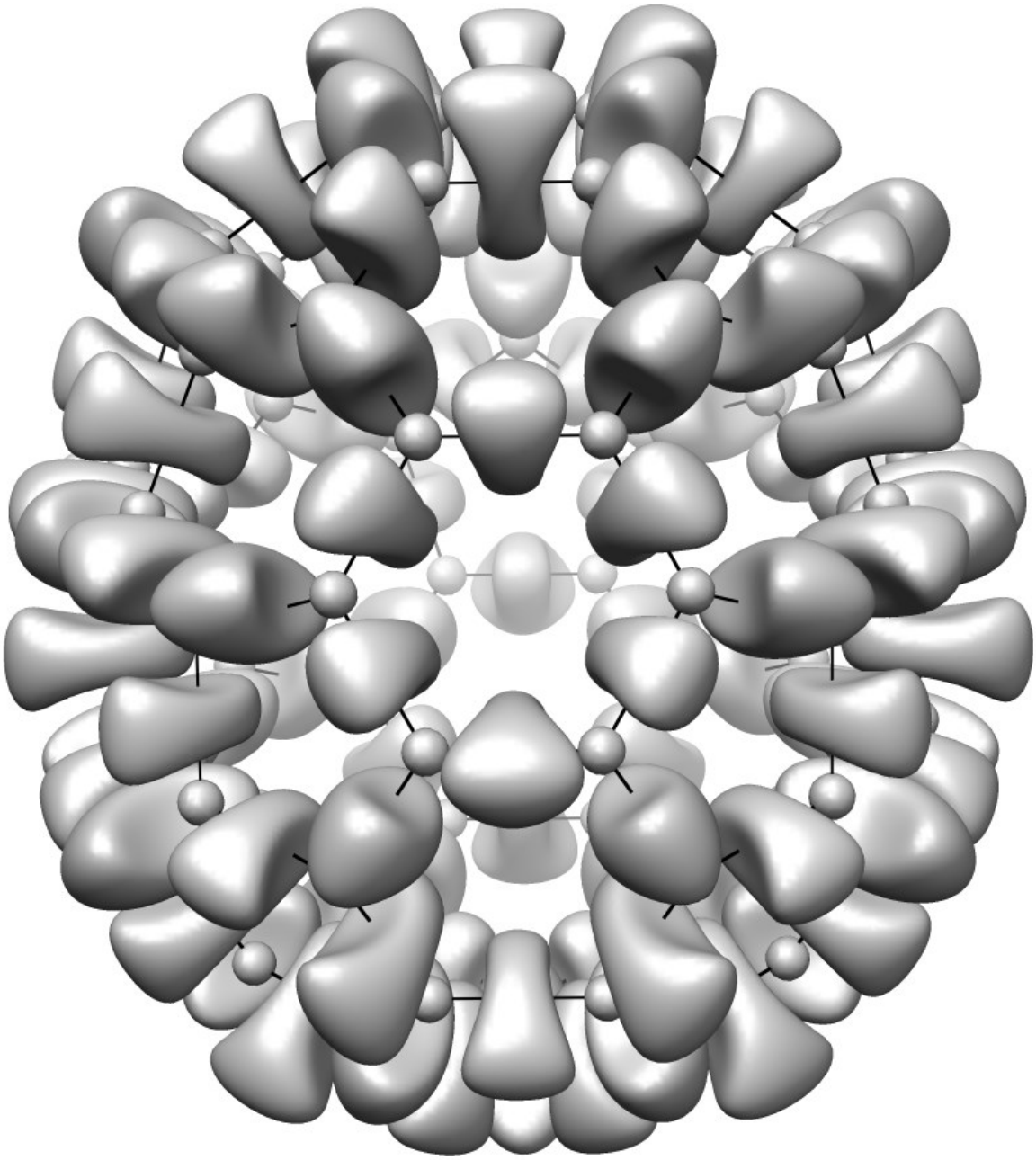

Describing the chemical bonding in C_{70} and $C_{70}O_3$ – a quantum chemical topology study.

Andrzej Bil,*[,a,b], Zdzisław Latajka,[b] Jürg Hutter,[a] Carole A. Morrison[c]

Supplementary materials

Table S1 Calculated properties of the carbon – carbon bonds bridged by O in the epoxides a,b-$C_{70}O$ and c,c- $C_{70}O$: R - equilibrium bond distance, V(C,C) - electron population of a valence ELI-D basin representing a bond, ρ – electron density at a bond critical point, Δρ – Laplacian of electron density at a bcp, ε – ellipticity of electron density at a bcp, H – energy density at a bcp.

	R/Å	V(C,C)	ρ/a.u.	Δρ/a.u.	ε	H/a.u.
C_a-C_a	1.54	1.67	0.218	-0.358	0.47	-0.178
C_a-C_b	1.53	1.68	0.224	-0.392	0.43	-0.188

Table S2 Calculated properties of selected carbon – carbon bonds in c,c-$C_{70}O_3$ in the vicinity of the ozone ring: R - equilibrium bond distance, V(C,C) - electron population of a valence ELI-D basin representing a bond, ρ – electron density at a bond critical point, Δρ – Laplacian of electron density at a bcp, ε – ellipticity of electron density at a bcp, H – energy density at a bcp.

	R/Å	V(C,C)	ρ/a.u.	Δρ/a.u.	ε	H/a.u.
C_b-C_c	1.52	2,12	0.254	-0.639	0.02	-0.219
C_a-C_b	1.37	3.13	0.325	-0.927	0.25	-0.347
C_b-C_c’	1.43	2.52	0.295	-0.801	0.16	-0.290
C_c-C_d	1.52	2.11	0.256	-0.653	0.03	-0.223
C_d-C_d	1.41	2.83	0.306	-0.838	0.21	-0.310
C_d-C_e	1.40	2.81	0.306	-0.849	0.20	-0.309

Table S3 Calculated properties of selected carbon – carbon bonds in a,b-$C_{70}O_3$ in the vicinity of the ozone ring: R - equilibrium bond distance, V(C,C) - electron population of a valence ELI-D basin representing a bond, ρ – electron density at a bond critical point, Δρ – Laplacian of electron density at a bcp, ε – ellipticity of electron density at a bcp, H – energy density at a bcp.

	R/Å	V(C,C)	ρ/a.u.	Δρ/a.u.	ε	H/a.u.
C_a'-C_a	1,52	2.12	0.251	-0.631	0.03	-0.214
C_b-C_c	1,524	2.109	0.252	-0.634	0.03	-0.216
C_a'-C_b'	1.373	3.111	0.324	-0.922	0.25	-0.344
C_a'-C_a''	1.431	2.543	0.288	-0.773	0.14	-0.280
C_c-C_c'	1.364	3.13	0.330	-0.952	0.25	-0.356
C_c-C_d	1.429	2.52	0.295	-0.805	0.16	-0.290

Table S4 Calculated properties of selected carbon – carbon bonds in e,e-$C_{70}O_3$ in the vicinity of the ozone ring: R - equilibrium bond distance, V(C,C) - electron population of a valence ELI-D basin representing a bond, ρ – electron density at a bond critical point, Δρ – Laplacian of electron density at a bcp, ε – ellipticity of electron density at a bcp, H – energy density at a bcp.

	R/Å	V(C,C)	ρ/a.u.	Δρ/a.u.	ε	H/a.u.
C_d-C_e	1.49	2.20	0.262	-0.678	0.05	-0.235
C_d-C_d	1.42	2.77	0.298	-0.802	0.20	-0.294
C_d-C_c	1.41	2.76	0.303	-0.827	0.20	-0.304

Table S5 The relative stabilities (ΔE) of the ozonide series and the perturbation of the population of V(C,C) basins (ΔN) upon ozonide formation.

	ΔE	ΔN		ΔE	ΔN
a,b-$C_{70}O_3$	0	4.74	b,c-$C_{70}O_3$	16.60	6.70
c,c-$C_{70}O_3$	2.03	4.94	a,a-$C_{70}O_3$	19.31	7.09
d,d-$C_{70}O_3$	6.75	6.43	c,d-$C_{70}O_3$	23.37	8.04
d,e-$C_{70}O_3$	16.50	6.47	e,e-$C_{70}O_3$	38.34	6.55

Figure S1 Changes in selected bond properties calculated for a,b-$C_{70}O_3$ vs. parent C_{70}. Differences in V(C,C) basins populations are plotted against left axis, while differences in bond distances (R), electron densities at the bcp (ρ), the Laplacian of the electron densities (Δρ), ellipticities (ε) and energy densities (H) are plotted against the right axis. The position of the relevant bonds against the C_a-C_b bond is presented in **Scheme S1**.

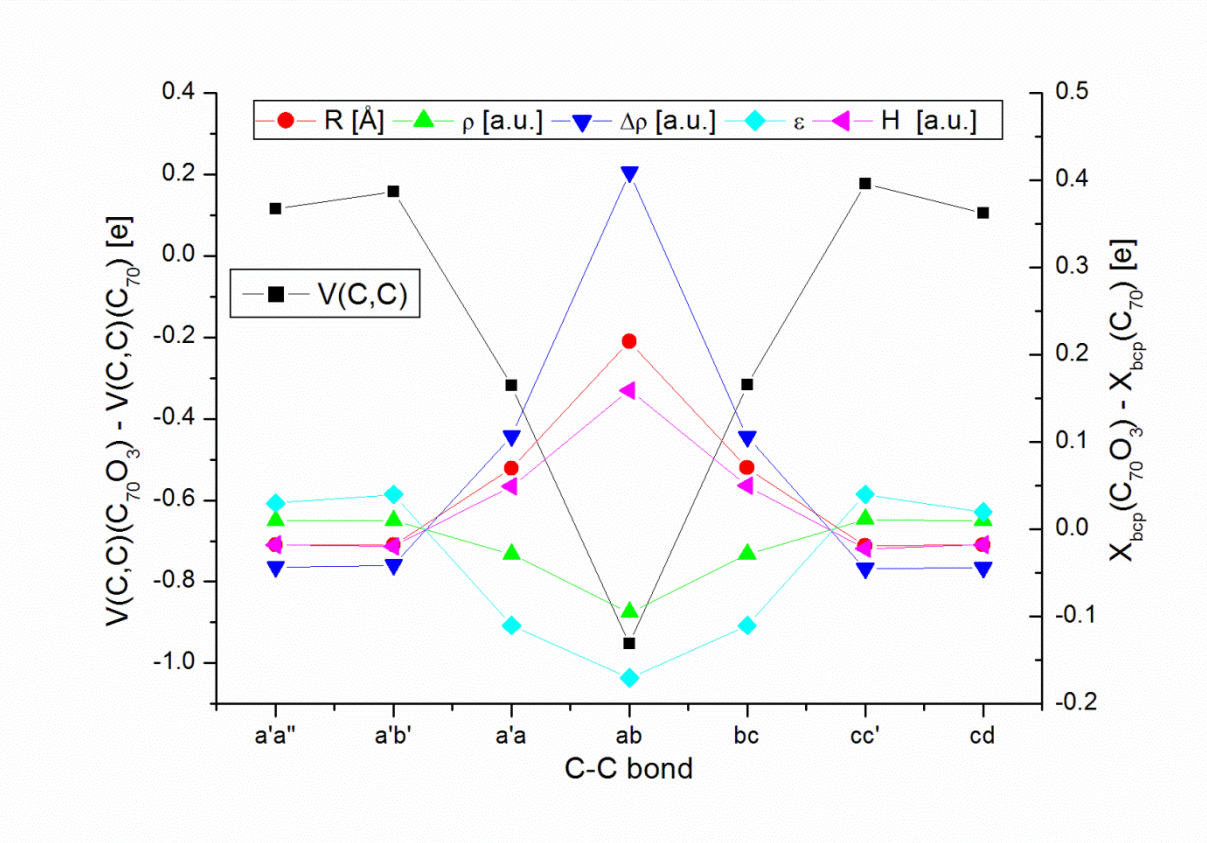

Scheme S1 Labeling of atoms relevant for Figure S1.

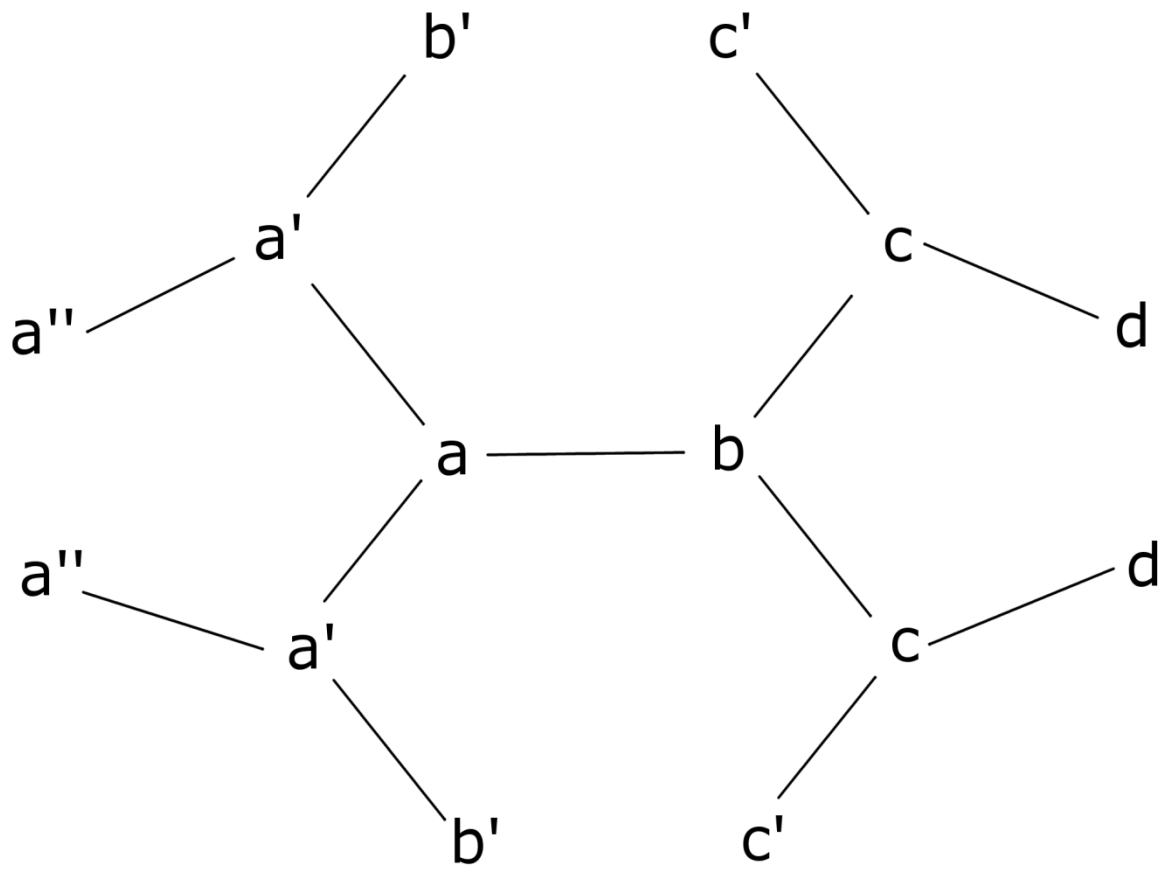

Figure S2 Changes in V(C,C) basins populations calculated for a,b-$C_{70}O_3$ vs. parent C_{70}. Upper panel represents C_a-C_a, C_a-C_b, C_b-C_c, C_c-C_c and C_c-C_d bonds in the hemisphere proximal to the ozone ring (up), lower panel is plotted for C_d-C_d and C_d-C_e bonds in the hemisphere proximal to the ozone ring, C_e-C_e bonds and all bonds in the distal hemisphere (down). All bonds for which the changes are greater than 0.1e are shown, along with information on how far they are from the ozone ring (i.e. one, two or three bonds from the ring).

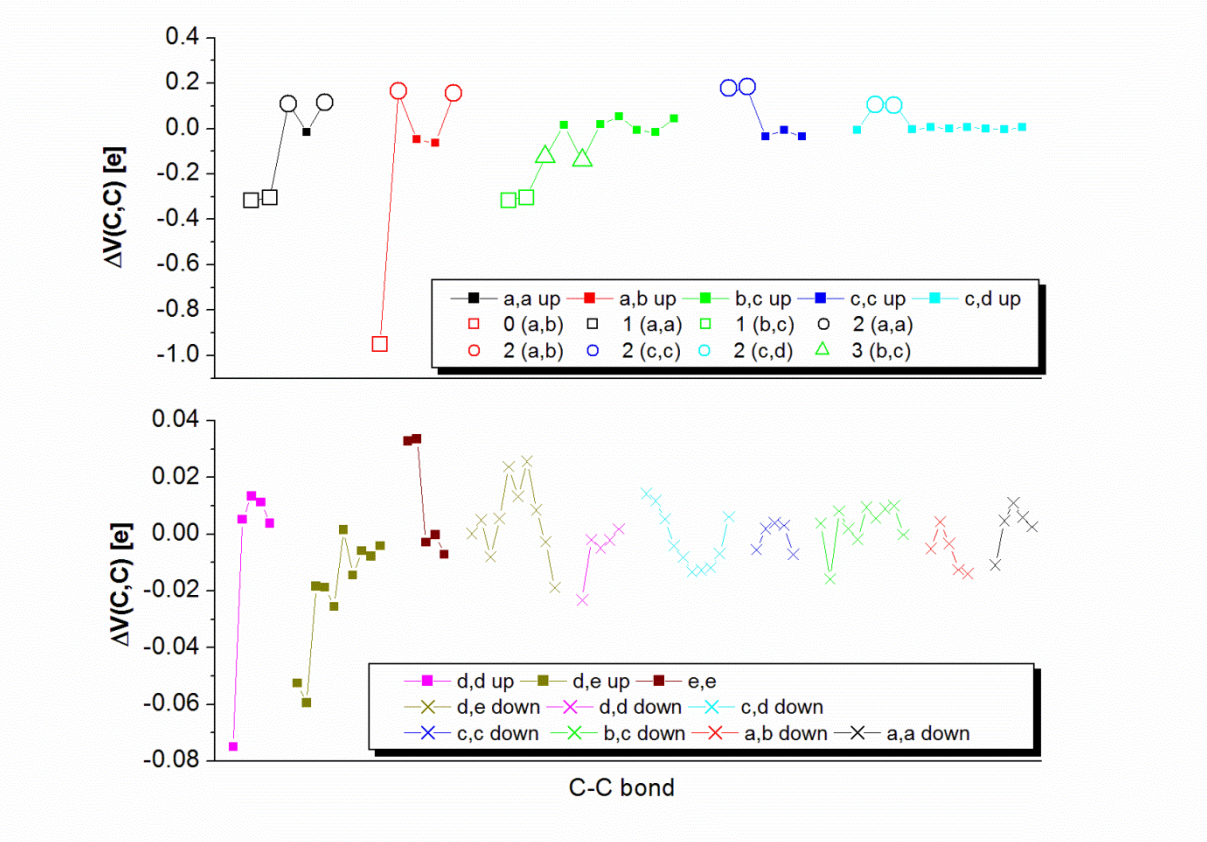

Figure S3 Changes in selected bond properties calculated for epoxide c,c-$C_{70}O$ vs. parent C_{70}.

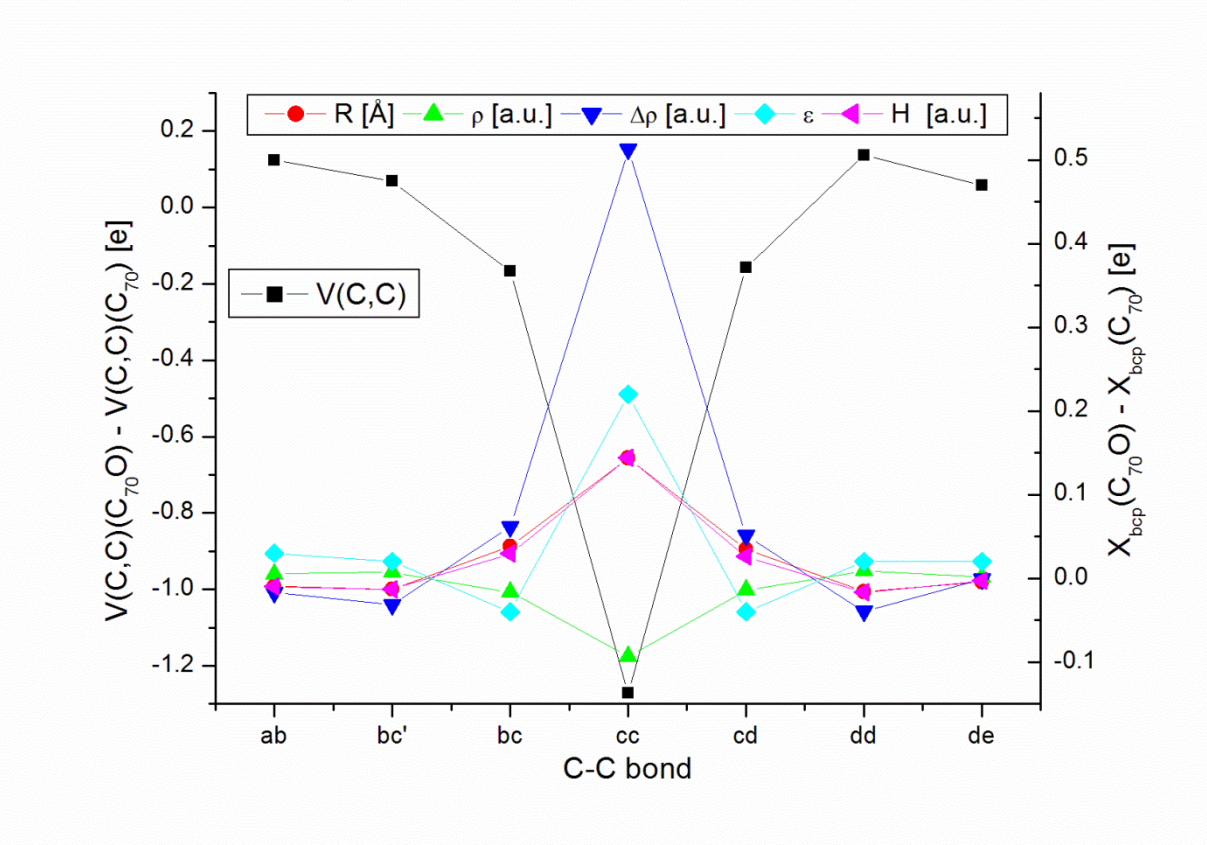

Figure S4 Changes in selected bond properties calculated for epoxide a,b-$C_{70}O$ vs. parent C_{70}.

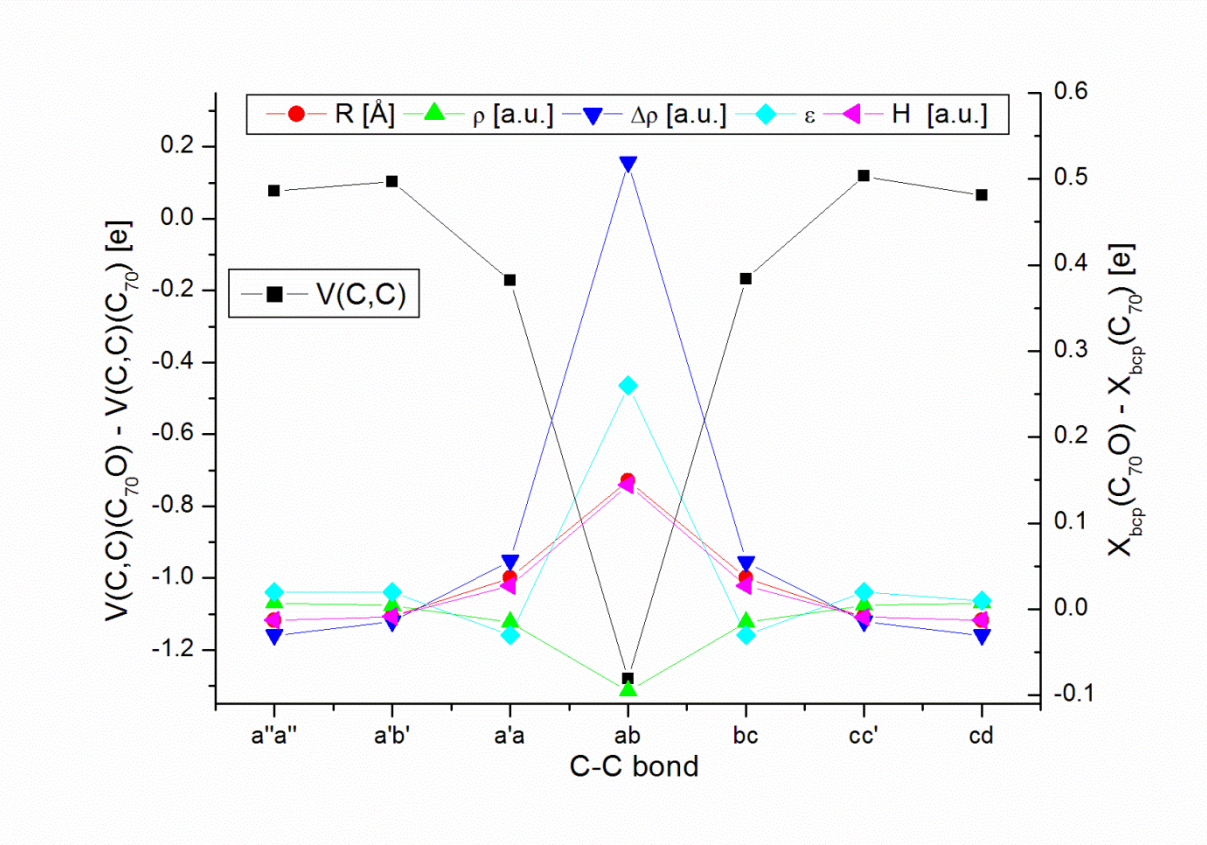

Figure S5 Changes in selected bond properties calculated for the oxidannulene e,e-$C_{70}O$ vs. parent C_{70}.

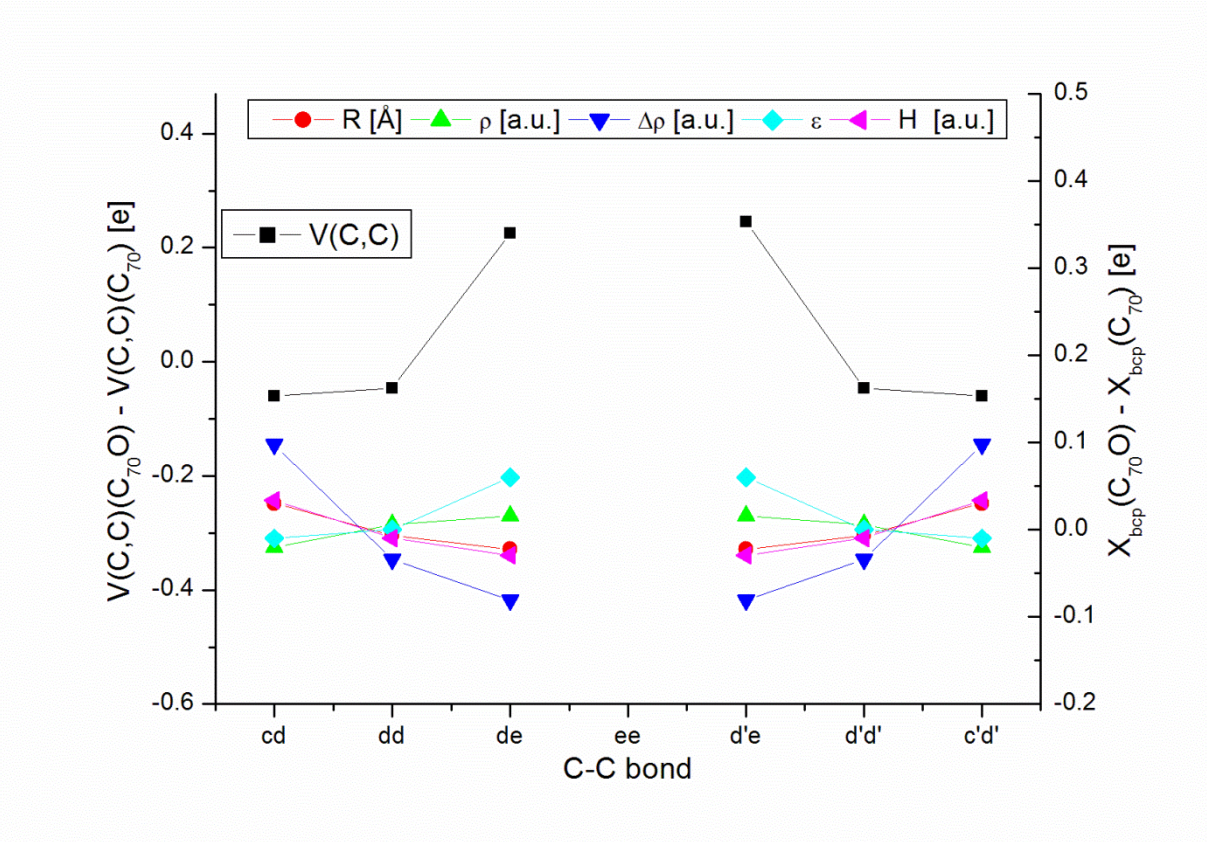

Figure S6 Changes in V(C,C) basins populations calculated for the epoxide c,c-$C_{70}O$ vs. parent C_{70}.

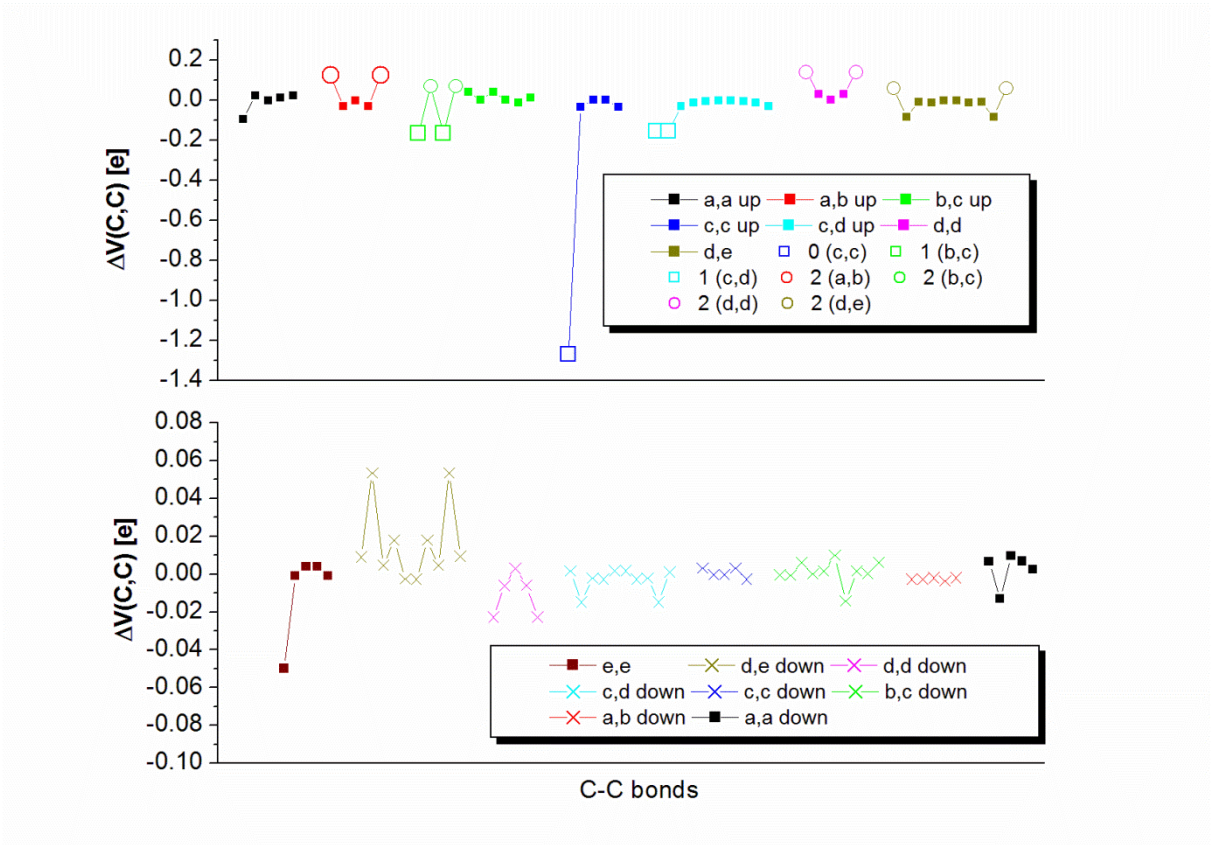

Figure S7 Changes in V(C,C) basins populations calculated for the epoxide a,b-$C_{70}O$ vs. parent C_{70}.

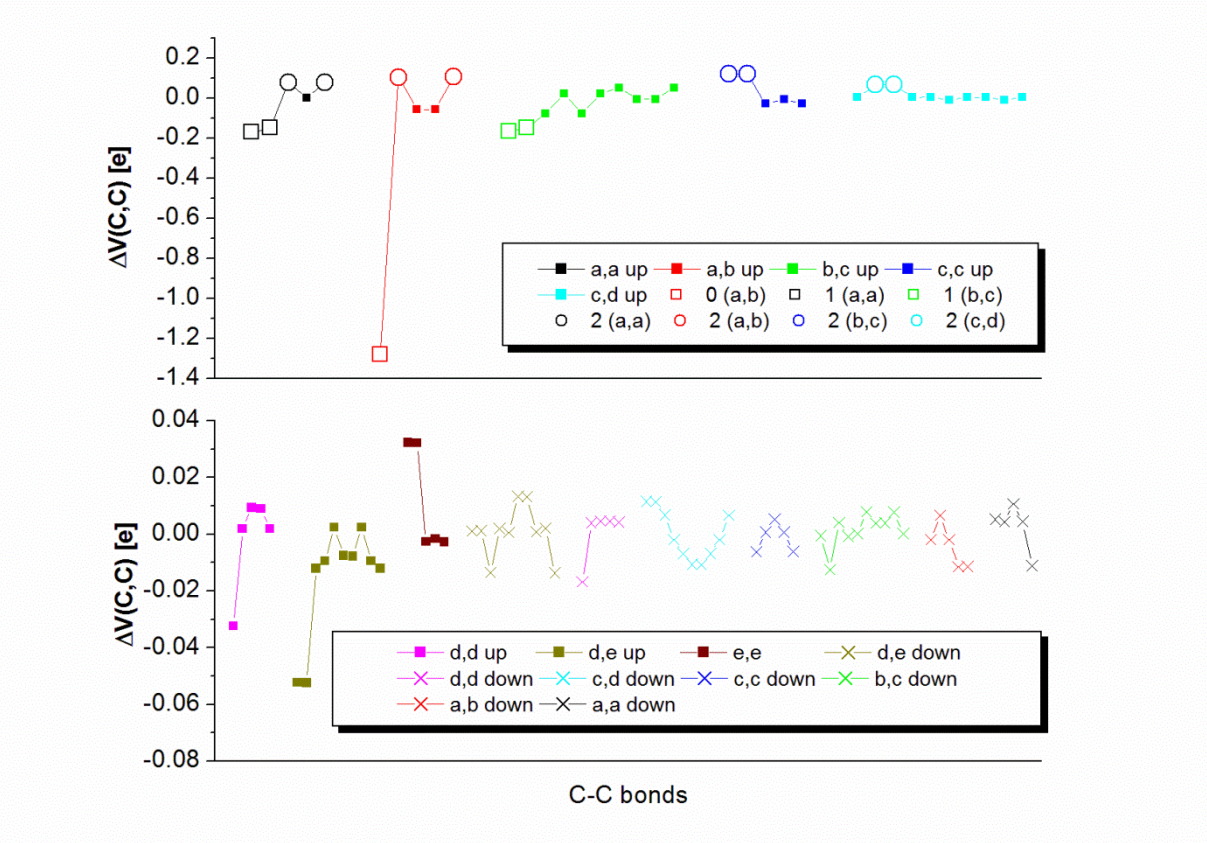

Figure S8 Changes in V(C,C) basins populations calculated for the oxidoannulene e,e-$C_{70}O$ vs. parent C_{70}.

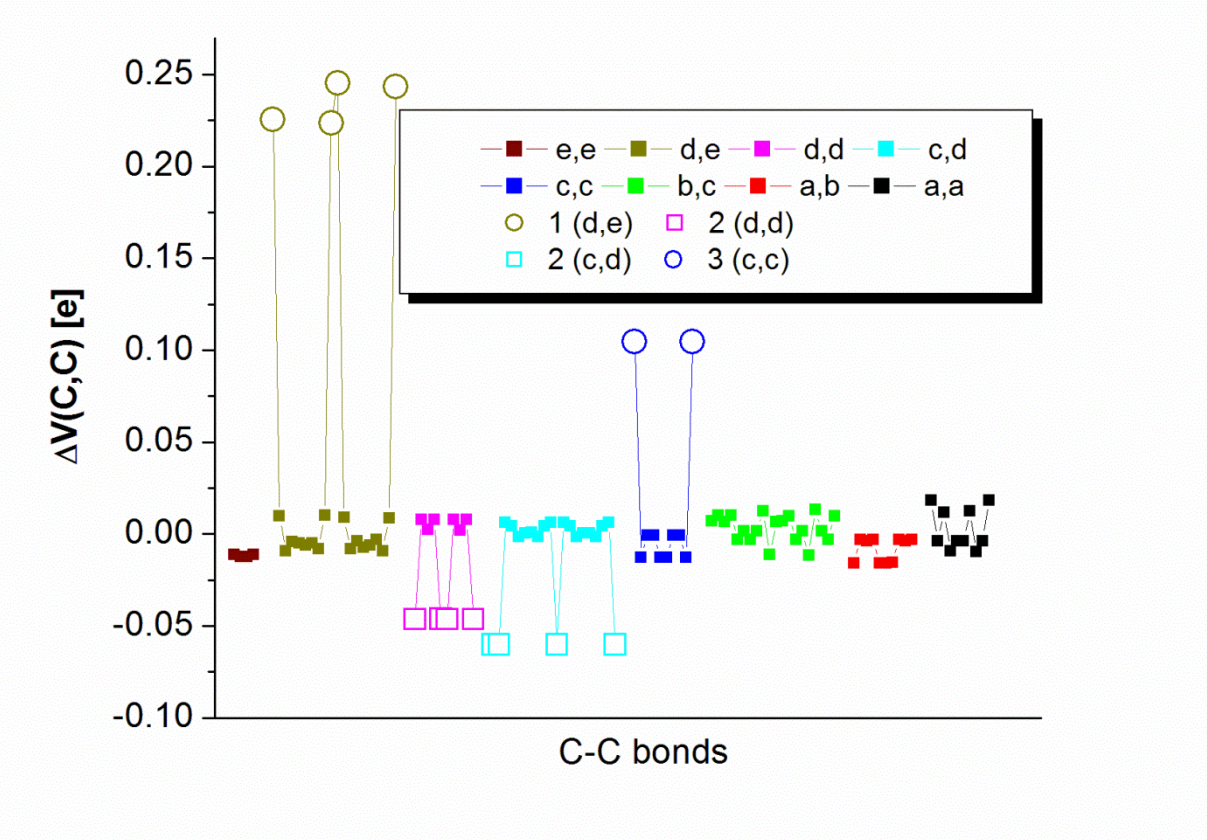

Figure S9 The minimum energy path, the evolution of the C-C and O-O bond distances (upper panel), and the evolution of the electron density at the (3,-1) critical points along with valence basin populations (lower panel) in the course of the ozone ring opening reaction for a,b-$C_{70}O_3$.